Geometric tail expectation in capital allocation: Asymptotic equivalence with conditional tail expectation and a case for advocacy

Takashi Owada*[1], Jianxi Su†[1], Zifu Wei‡[3,1], and Zhongyi Yuan§[2]

[1]Department of Statistics, Purdue University, West Lafayette, IN 47907, USA

[2]Smeal College of Business, The Pennsylvania State University, State College, PA 16801, USA

[3]School of Economics, Sichuan University, Chengdu, China

Abstract

Risk measure and capital allocation are arguably two of the most important notions in quantitative risk management. They are closely related, as the former often shapes how the latter is implemented. In this paper, we conduct an asymptotic analysis of a proportional risk allocation derived using the geometric tail expectation (GTE) risk measure. As a relative and robust variant of the widely adopted conditional tail expectation (CTE) risk measure, the GTE risk measure has garnered increasing attention in recent literature. It induces a proportional allocation that can be regarded as a stochastic counterpart of the deterministic composition that underlies the CTE-induced proportional allocation. Our asymptotic analysis reveals that, across various tail scenarios, the CTE-based and GTE-based allocation methods essentially converge when the confidence level is sufficiently high. This is a welcome finding, since it reconciles discrepancies among risk analysts regarding the selection between the absolute-term CTE risk measure and the relative-term GTE risk measure for risk allocation purposes. Moreover, the asymptotic equivalence supports advocating for the use of GTE-based allocation as a more versatile alternative to the CTE-based allocation, in the sense that the GTE-based allocation is always well-defined while the CTE-based allocation is not. Our simulation example also indicates that, under scenarios with heavy-tailed distributions and strong dependence structures, the empirical estimator of the GTE-based allocation may exhibit significantly smaller variance compared with that of the CTE-based allocation.

Keywords: Risk analysis, capital allocation, heavy tail, tail dependence, stochastic risk contribution

*Postal address: 150 N. University Street, West Lafayette, IN 47907, U.S.A.; email: owada@purdue.edu

†Postal address: 150 N. University Street, West Lafayette, IN 47907, U.S.A.; email: jianxi@purdue.edu

‡Postal address: No.24, South Section 1, Yihuan Road, Chengdu, Sichuan, China; email: zifuwei@scu.edu.cn

§Corresponding author; postal address: 362 Business Building, University Park, PA 16802, U.S.A.; email: zuy11@psu.edu

1 Introduction

Within the encompassing framework of quantitative risk management in insurance, two foundational objectives involve the determination of economic capital and its subsequent allocation. Holding adequate economic capital is important for insurance companies to absorb excessive losses caused by shock events. Determining the required economic capital typically entails assessing the level of aggregate risk across all key risk factors to which a company is exposed. While closely related, this paper focuses on the latter notion—capital allocation—which involves developing a meaningful scheme for apportioning the total economic capital back to the constituent business units (BUs). Effective capital allocation serves multiple business purposes, including risk-based pricing, profitability analysis, risk sharing, and risk budgeting (see a comprehensive discussion in Guo et al., 2021).

A wide variety of capital allocation principles have been proposed and studied in the literature, yet many ultimately fall under the umbrella of Euler's allocation framework (Kalkbrener, 2005). In particular, what arguably stands out as one of the most popular choices among practitioners is the Euler allocation induced by the conditional tail expectation (CTE)—a risk measure that has been included into the recent regulatory accords. Consequently, the study of the CTE-based allocation has attracted considerable scholarly attention. Beyond its roots in Euler's allocation, the CTE-based allocation can also be constructed through the Aumann-Shapley allocation (Denault, 2001), distorted allocation (Tsanakas and Barnett, 2003), and weighted allocation (Furman and Zitikis, 2008). Moreover, it has been shown to be optimal under specific mathematical criteria, as demonstrated by Laeven and Goovaerts (2004) and Dhaene et al. (2012).

Related to the literature on the CTE-based allocation, this paper investigates a newly developed capital allocation method, which is formulated as the conditional expectation of the stochastic risk contribution of an individual BU to the aggregate risk, given that the risk portfolio is stressed under a tail scenario (Bauer and Zanjani, 2016; Furman et al., 2021). We refer to this method as the geometric tail expectation (GTE) based allocation, because it is derived as the Euler allocation induced by the GTE risk measure (Mohammed et al., 2021). The GTE belongs to the class of return risk measures which provide relative assessments of risk, in contrast to monetary risk measures, which offer absolute assessments of risk (Bellini et al., 2018; Laeven et al., 2024; Laeven and Rosazza Gianin, 2022). More specifically, according to the correspondence proposed by Bellini et al. (2018), the GTE is the relative, return risk measure counterpart of the CTE, which is a monetary risk measure.

Furthermore, the use of the GTE risk measure for capital allocation can be also motivated by the risk measure reverse-engineered by Bauer and Zanjani (2016). Specifically, for a profit-maximizing insurer operating in an incomplete market with risk-averse counterparties, they derived a risk measure desirable for the capital allocation purpose. The risk measure they obtained closely resembles the GTE. Thus, another compelling motivation for

studying GTE-based capital allocation arises from the contrast between the preferences of profit-oriented insurers, who may favor the GTE for its alignment with economic fundamentals, and the regulator's endorsement of CTE, which is grounded in the notion of prudence.

In this paper, we aim to study the asymptotic behavior of the GTE-based allocation as the associated confidence level parameter q approaches one. The insurance industry's best practice that emphasizes prudent risk assessment motivates our asymptotic approach. For instance, in both regulatory and internal risk management applications, in order to account for extreme but plausible loss scenarios, the confidence level q used in risk metrics such as Value-at-Risk (VaR) and CTE is usually set close to 1. Consequently, a large body of literature has been devoted to the asymptotic estimates of tail-based risk measures (Cui et al., 2024; Hua and Joe, 2012; Mao et al., 2023; Zhu and Li, 2012b), as well as the capital allocation rules they induce (Asimit and Badescu, 2010; Chen and Liu, 2022, 2024; Qin and Zhou, 2021; Zhu and Li, 2012a). We contribute to the aforementioned literature through an asymptotic analysis of the GTE-based allocation, which has not yet been explored.

Here is a preview of our research. We carry out an asymptotic analysis of the GTE-based allocation under a comprehensive set of tail risk scenarios that account for both heavy-tailed and light-tailed risks, as well as both tail-dependent and tail-independent structures. We derive the limit of the GTE-based allocation as the confidence level parameter $q \uparrow 1$, and compare it to the asymptotic behavior of the CTE-based allocation, which is now widely adopted in practice. Remarkably, across all the tail risk scenarios considered, we find that the two allocation methods are asymptotically equivalent. It is noteworthy that even though our results are derived through asymptotic analysis, we show through extensive numerical examples that, under various scenarios, the findings largely hold when q reaches 95%.

This theoretical finding carries notable practical implications. To be specific, the difference between the CTE-based and GTE-based allocation methods arises from the use of the two different risk measures in deriving the respective Euler allocation rules. Whether one argues from mathematical principles (Laeven and Rosazza Gianin, 2022) or business fundamentals (Bauer and Zanjani, 2016; Mohammed et al., 2021), the choice of risk measure for the allocation rule remains subjective. The asymptotic equivalence elucidated in this study serves to reconcile the discrepancies among risk analysts' divergent perspectives regarding the selection between the regulatory CTE risk measure and its relative counterpart, the profit-maximizion motivated GTE risk measure, for capital allocation purposes. A similar problem was also studied by Mohammed et al. (2021), who characterized the class of risk portfolios for which the parity between the CTE-based and GTE-based allocations holds across the entire range of confidence level $q \in [0,1)$. Our study shows that by relaxing this requirement to a more practically relevant setting where only confidence levels close to 1 are considered, this desirable equivalence holds for a substantially broader class of risk portfolios.

Further, the asymptotic parity developed provides a strong support for adapting the newly developed GTE-based allocation as a more versatile alternative to the currently widely adopted CTE-based allocation. Firstly, when empirical estimators (e.g., Gribkova et al., 2022b) are employed to calculate these allocations from data, our numerical study shows that when the tails of marginal distributions are heavy and tail dependencies are strong, the estimator of the GTE-based allocation demonstrates greater statistical robustness in terms of lower estimation variance, in comparison to that of the CTE-based allocation.

Additionally, the CTE risk measure only exists for loss random variables (RVs) with finite mean. For this reason, the literature on the CTE-based allocation for heavy-tailed risks has to restrict to the cases where the tail indices are greater than one, whereas the GTE-based allocation is always well defined and not subject to the restriction. Note that the presence of infinite means that preclude the use of the CTE-based allocation reflects a non-trivial phenomenon and has drawn substantial interest in both applied and theoretical research. Among some notable contributions, Moscadelli (2004) and Chavez-Demoulin et al. (2016) found that the operational risk losses in their datasets exhibit infinite means; Malavasi et al. (2022), in accordance with other studies in cyber loss modeling, found that cyber related loss distributions are of infinite mean across business sectors and risk categories; Chen et al. (2025) investigated stochastic dominance and the implications for risk diversification under infinite-mean models. See also Chen and Wang (2025) for a comprehensive review of recent advances in infinite-mean models in risk management. Admittedly, some studies favoring infinite-mean models obtain tail index estimates near the boundary between the finite-mean and infinite-mean regimes, inevitably leaving the conclusions open to debate. Nonetheless, our point is that, since determining whether the "true" model has a finite or infinite mean can be challenging, it is desirable to have a method capable of handling both the finite-mean and infinite-mean cases.

Taken together, this paper conveys the following practical messages. On the one hand, for risk analysts who favor the CTE-based allocation, its asymptotic equivalence with the GTE-based allocation not only bridges the conceptual divide between absolute risk assessments via monetary risk measures such as the CTE and relative risk assessments via return risk measures such as the GTE, but also reconciles regulatory prudence with economic desirability in the context of capital allocation. Specifically, the asymptotic equivalence offers an alternative, economically grounded justification for the CTE-based method, framed through the lens of profit maximization, which originally motivated the development of the GTE-based allocation (Bauer and Zanjani, 2016; also see discussions in Mohammed et al., 2021). On the other hand, for those open to selecting between the CTE-based and GTE-based approaches, the asymptotic equivalence between the two methods, together with the statistical considerations discussed earlier, provides a compelling case for favoring the GTE-based allocation.

The connection as well as the sharp contrast between the CTE and GTE risk measures motivate the undergoing of our paper are illustrated in Figure 1. The figure highlights how the derived asymptotic equivalence between

the two allocation methods serves to reconcile these seemingly divergent perspectives: absolute versus relative assessments of risk, and regulatory conservatism versus profit-oriented motive. The mathematical expressions shown in Figure 1 will be further elaborated in the subsequent section.

RM	Motivation	RM Classification	Assessment Classification
CTE	Regulator's endorsement	Monetary RM	Absolute
GTE	Profit maximization	Return RM	Relative

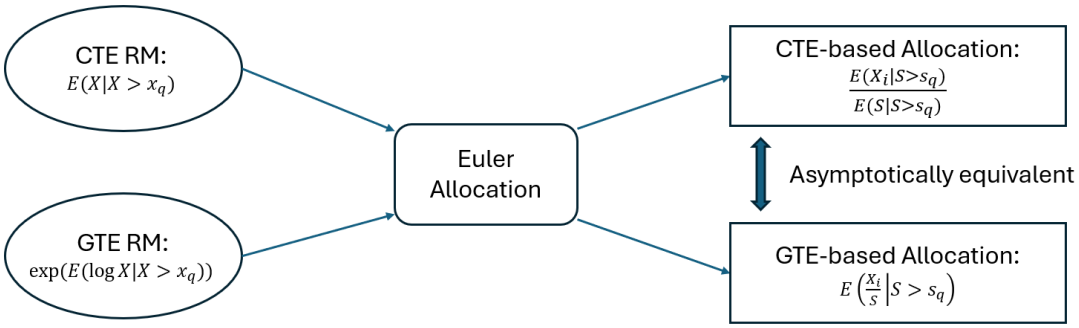

Figure 1: Summary of the connection as well as the sharp contrast between the CTE and GTE risk measures (abbreviated as "RM" in the figure) and the asymptotic equivalence result that reconciles the two.

The rest of the paper is organized as follows. Section 2 formally defines capital allocation as well as the GTE-based method, whose asymptotic analysis forms the main focus of this paper. Section 3 introduces some standard notation and terminologies relevant to asymptotic analysis. Sections 4 and 5 examine the asymptotic behavior of the GTE-based allocation under the assumptions of asymptotic dependence and asymptotic independence, respectively. Sections 6 and 7 illustrate our findings using, respectively, simulated data and real-world data. Finally, Section 8 concludes the paper.

2 Capital allocation and the proportional scheme induced by the geometric tail expectation risk measure

Throughout this paper, we work with an atomless and rich probability space $(\Omega, \mathcal{F}, P)$. We confine ourselves to a setting where risk RVs are assumed to be non-negative. Such a setting is rather typical in insurance risk management, although we acknowledge that in broader financial contexts, capital allocation may be defined more generally over real-valued RVs. To this end, we define $\mathcal{X} := \{X : \Omega \to [0,\infty) \,|\, X \text{ is } \mathcal{F}\text{-measurable}\}$ as the collection of non-negative risk RVs relevant to the study in this paper. Consider a risk portfolio consisting of $n \in \mathbb{N}$ BUs, and let the i-th component of $\boldsymbol{X} = (X_1, \ldots, X_n) \in \mathcal{X}^n$ represent the risk associated with the i-th BU, $i \in \mathcal{N} = \{1, \ldots, n\}$.

Motivated by the setup in Dhaene et al. (2012); Fiori and Rosazza Gianin (2025); Furman et al. (2021), we assume that the total capital is predetermined and fixed prior to allocation. Accordingly, the capital allocation exercise is formulated via a *proportional* allocation scheme:

$$\big\{r_i \in [0,1]\big\}_{i=1,\dots,n} \quad \text{such that } \textstyle\sum_{i=1}^n r_i = 1, \tag{1}$$

where r_i denotes the proportion of risk capital allocated to BU i, and the latter condition ensures that the total capital is fully allocated. Such a two-step approach to determining allocated capital aligns with regulatory considerations, e.g., the NAIC risk-based capital framework (NAIC, 2012) or the Own Risk and Solvency Assessment (OSFI, 2017), where the total risk capital is first assessed based on key risk factors (e.g., market, insurance, and credit risks), and then subsequently allocated to individual BUs.

To introduce the capital allocation methods relevant to the discussions in this current paper, let us begin by recalling the CTE-based allocation. Let $S = X_1 + \cdots + X_n$ denote the aggregate risk RV associated with the risk portfolio $\boldsymbol{X}$. Then the CTE-based allocation is formulated as

$$\mathrm{CTE}_q(X_i, S) := E(X_i \,|\, S > s_q), \qquad i \in \mathcal{N},\ q \in [0,1), \tag{2}$$

where $s_q = \inf\big\{s > 0 : P(S \le s) > q\big\}$ represents the VaR of the aggregate risk S. Correspondingly, the CTE-based *proportional* allocation is given by

$$r_{i,q} := \frac{\mathrm{CTE}_q(X_i,S)}{\sum_{i=1}^n \mathrm{CTE}_q(X_i,S)} = \frac{\mathrm{CTE}_q(X_i,S)}{\mathrm{CTE}_q(S)}, \qquad i \in \mathcal{N},\ q \in [0,1), \tag{3}$$

where $\mathrm{CTE}_q(X) := \mathrm{CTE}_q(X,X)$, $X \in \mathcal{X}$, denotes the CTE risk measure.

Note that the allocation problem described in equation (1) indicates an inherent connection with the notion of risk composition/contribution (Belles-Sampera et al., 2016; Boonen et al., 2019; Furman et al., 2021). Specifically, let $\boldsymbol{x} = (x_1, \dots, x_n)$, $s = x_1 + \cdots + x_n$, and denote by $C_i(\boldsymbol{x}) = x_i/s$ the composition function, $i \in \mathcal{N}$. The CTE-based proportional allocation (3) can be regarded as

$$r_{i,q} = C_i\big(\mathrm{CTE}_q(X_1,S), \dots, \mathrm{CTE}_q(X_n,S)\big) \qquad i \in \mathcal{N},\ q \in [0,1). \tag{4}$$

The CTE-based proportional allocation in (4) should be viewed as a deterministic composition approach for evaluating risk contribution. A stochastic composition alternative to (4), which is perhaps more natural to interpret

from a probabilistic standpoint, can be given by

$$\tilde{r}_{i,q} := E(R_i \,|\, S > s_q), \qquad i \in \mathcal{N},\ q \in [0,1), \tag{5}$$

where

$$R_i = C_i(\boldsymbol{X}) = \frac{X_i}{S}, \qquad i \in \mathcal{N}, \tag{6}$$

denotes the relative, stochastic contribution of the risk attributed to the i-th BU (Bauer and Zanjani, 2016; Furman et al., 2021). Akin to the CTE-based allocation, $\tilde{r}_{i,q}$ defined in (5) can also be constructed as an Euler proportional allocation, but it is induced by the GTE risk measure (Bauer and Zanjani, 2016; Mohammed et al., 2021):

$$\mathrm{GTE}_q(X) := \exp\left\{E\left(\log X \,|\, X > x_q\right)\right\}, \qquad X \in \mathcal{X},\ q \in [0,1), \tag{7}$$

which is a relative, return-based counterpart of the CTE risk measure (Bellini et al., 2018; Laeven and Rosazza Gianin, 2022). This justifies referring to $\tilde{r}_{i,q}$ in (5) as the GTE-based allocation.

In contrast to the extensive literature on the CTE risk measure and its associated allocation methods, relatively few results have been established for the aforementioned newly developed GTE-based allocation rule described in equation (5), which serves as the primary focus of this paper. To be specific, we will conduct an asymptotic analysis of the GTE-based allocation $\tilde{r}_{i,q}$ as $q \uparrow 1$ under tail assumptions that are inspired by Asimit et al. (2011), who carried out a similar analysis for the CTE-based allocation.

It is noteworthy that the CTE-based allocation (3) and the GTE-based allocation (5) are mathematically similar. While the former entails the composition of conditional expectations, the latter relies on the conditional expectation of stochastic risk composition. At first glance, one might expect that changing the order of composition and conditional expectation would generally lead to different allocation outcomes. Rather surprisingly, as we establish the limiting behavior of $\tilde{r}_{i,q}$ in the remainder of this article, we find that the two allocation methods (3) and (5) are asymptotically equivalent when the confidence level q is sufficiently close to one.

3 Technical preliminaries

This section contains some preliminaries on extreme value theory (EVT) and tail analysis. We start by listing our notational convention.

3.1 Notational convention

Throughout this paper, we denote the distribution functions of X_i by F_i and its survival function by $\overline{F}_i$, $i \in \mathcal{N}$. When no confusion could arise, for a positive integer n, we denote $[0,\infty)^n$ by $[\mathbf{0},\boldsymbol{\infty})$ or $\mathbb{R}_+^n$ and $[-\infty,\infty)^n$ by $[-\boldsymbol{\infty},\boldsymbol{\infty})$ or $\mathbb{R}^n$, and likewise, shorthand $(x_1,\infty)\times\ldots\times(x_n,\infty)$ by $(\boldsymbol{x},\boldsymbol{\infty})$, where $\boldsymbol{x}=(x_1,\ldots,x_n)\in\mathbb{R}^n$. Vector operations such as $\boldsymbol{x}+\boldsymbol{y}$, $c\boldsymbol{x}$, and $\boldsymbol{x}>\boldsymbol{y}$ for $\boldsymbol{x},\boldsymbol{y}\in\mathbb{R}^n$ and $c\in\mathbb{R}$ are to be understood component wise.

Denote by $\mathbb{C}$ a cone in $\mathbb{R}^n$, which, by definition, is closed under positive scale multiplication, and by $\mathbb{C}_0$ a closed cone in $\mathbb{C}$. Denote by $\mathbb{M}(\mathbb{C}\setminus\mathbb{C}_0)$ the set of all Borel measures on $\mathbb{C}\setminus\mathbb{C}_0$ that assign finite measure to Borel subsets bounded away from $\mathbb{C}_0$. For a measure $\mu\in\mathbb{M}(\mathbb{C}\setminus\mathbb{C}_0)$ and a measurable set $A\subset\mathbb{C}\setminus\mathbb{C}_0$, we may write $\mu(A)$ as μA when there is no confusion.

All limits are taken as t tending to ∞ unless otherwise stated.

3.2 EVT, regular variation, $\mathbb{M}$ convergence, and tail dependence

Let us first recollect a fundamental result in EVT, the Fisher-Tippett-Gnedenko theorem. It states that if a distribution F is in the maximum domain of attraction (MDA) of some non-degenerate distribution G, namely, there exist some $a_m>0$ and $b_m\in\mathbb{R}$, $m=1,2,\ldots$, such that $\lim_{m\to\infty}F^m(a_mx+b_m)=G(x)$, $x\in\mathbb{R}$, then G must be a Fréchet distribution, a Weibull distribution, or a Gumbel distribution. While distributions in the Weibull case have finite upper end points, those in the MDA of the Fréchet and Gumbel distributions often have unbounded right tails. In the context of quantitative risk management, the calculations of economic capital and its allocation primarily rely on the joint behavior of BUs in their right tails, often assumed to be unbounded, particularly for tail risk analysis. Thus, in our paper we are going to focus on the Fréchet and Gumbel cases.

A distribution function F in the MDA of the Fréchet distribution, written as $F\in\mathrm{MDA}(\Phi)$, is known to have a regularly varying tail, in the sense that

$$\lim_{t\to\infty}\frac{\overline{F}(xt)}{\overline{F}(t)}=x^{-\alpha},\qquad x>0, \tag{8}$$

for some $\alpha>0$. In this case, the tail of the distribution is known to decay at a power rate. We write $\overline{F}\in\mathrm{RV}_{-\alpha}$. If equation (8) holds with $\alpha=\infty$, then we write $\overline{F}\in\mathrm{RV}_{-\infty}$.

A distribution function F with right endpoint $t_F:=\sup\{x\in\mathbb{R}:\overline{F}(x)>0\}$ is said to be in the MDA of the Gumbel distribution, written as $F\in\mathrm{MDA}(\Lambda)$, if and only if there exists a positive function $a(\cdot)$ such that $a(t)=o(t)$ and

$$\lim_{t\uparrow t_F}\frac{\overline{F}(t+xa(t))}{\overline{F}(t)}=e^{-x},\qquad x\in\mathbb{R}. \tag{9}$$

In tail risk analysis, we are less concerned with bounded risks and hence in this paper we only focus on the case with $t_F = \infty$ and assume that is the case for every individual risk in portfolio $\boldsymbol{X}$. Note that, the auxiliary function $a(t)$ is self-neglecting, with $\lim_{t\to\infty} a(t+a(t)x)/a(t) = 1$ holding locally uniformly.

To define regular variation for a random vector, we introduce the concept of $\mathbb{M}$ convergence (or, equivalently, $\mathbb{M}^*$ convergence). In general, for a sequence of measures μ and $\{\mu_i\}_{i\geq 1}$ in $\mathbb{M}(\mathbb{C}\setminus\mathbb{C}_0)$, we say

$$\mu_n \to \mu \qquad \text{in } \mathbb{M}(\mathbb{C}\setminus\mathbb{C}_0) \tag{10}$$

as $n\to\infty$ if $\lim_{n\to\infty}\int_{\mathbb{C}} f\mathrm{d}\mu_n = \int_{\mathbb{C}} f\mathrm{d}\mu$ holds for any f that is a continuous and bounded function on $\mathbb{C}\setminus\mathbb{C}_0$ with support bounded away from $\mathbb{C}_0$. It is known that the $\mathbb{M}$ convergence in (10) is equivalent to the condition that

$$\lim_{n\to\infty}\mu_n(A) = \mu(A) \tag{11}$$

for every Borel subset A bounded away from $\mathbb{C}_0$ such that the boundary of A is μ negligible; that is, $\mu(\partial A) = 0$. The closed cone $\mathbb{C}_0$ is called a forbidden zone and a region bounded away from $\mathbb{C}_0$ is considered as a tail region. In this paper, we focus on the case with $\mathbb{C}_0 = \{\mathbf{0}\}$ and $\mathbb{C}$ is either $\mathbb{R}^n_+$ or $\mathbb{R}^n$.

Note that there is no standard analogy that characterizes random vectors with marginal distributions in the MDA of the Gumbel distribution through convergence of measures in a metric space. Nonetheless, the structure given in Assumption 2.2 of Asimit et al. (2011) provides a resembling characterization and will be our modeling choice for this paper.

It is well known that tail dependence is a major factor that impacts risk capital allocation. Naturally, we shall consider both asymptotically dependent risks and asymptotically independent risks. A pair of risks X_i and X_j with cumulative distribution functions F_i and F_j respectively, are said to be asymptotically dependent if

$$\liminf_{q\uparrow 1} P\big(F_i(X_i) > q \,|\, F_j(X_j) > q\big) > 0. \tag{12}$$

We use the terms tail dependence and asymptotic dependence interchangeably. Asymptotic dependence for the multivariate cases considered later will entail different forms, but are natural extensions of (12).

4 Asymptotically dependent portfolios

We begin by analyzing a portfolio of asymptotically dependent risks, considering two scenarios: one with Fréchet tails and the other with Gumbel tails.

4.1 Fréchet case

For the case where the risks have Fréchet tails, we use the multivariate regular variation (MRV) structure to model the risks. MRV is an integrated structure that models both the marginal distributions with regularly varying tails and their tail dependence. In this paper, we use the notion of $\mathbb{M}$ convergence to define MRV.

($\mathbf{C}_1$) The nonnegative risk vector $\boldsymbol{X}$ possesses MRV; that is, for some nonzero and nondegenerate measure μ, it holds that

$$\frac{P(\boldsymbol{X}/t \in \cdot)}{\overline{F}_1(t)} \to \mu \qquad \text{in } \mathbb{M}\left(\mathbb{R}_+^n \setminus \{\mathbf{0}\}\right). \tag{13}$$

Moreover, the limit measure μ assigns positive mass to the interior; that is, $\mu(\mathbf{0}, \boldsymbol{\infty}) > 0$.

Note that the condition $\mu(\mathbf{0}, \boldsymbol{\infty}) > 0$ ensures that the risks are asymptotically dependent and, because of the homogeneity of the limit measure μ, is equivalent to the condition that $\mu(\boldsymbol{x}, \boldsymbol{\infty}) > 0$ for some $\boldsymbol{x} > \mathbf{0}$.

It is noteworthy that, traditionally, MRV is defined through vague convergence of Radon measures (Resnick, 2007). However, a recent trend in the literature is to define MRV through $\mathbb{M}$ convergence of measures that are finite on sets bounded away from a designated forbidden zone, which is simply $\{\mathbf{0}\}$ in relation (13). An advantage of formulating MRV using $\mathbb{M}$ convergence is that compactification of the space—which causes problems with polar coordinate transformation—is no longer needed. As an example, to define regular variation of a nonnegative n-dimensional random vector, compactificiation of $[\mathbf{0}, \boldsymbol{\infty})$ into $[\mathbf{0}, \boldsymbol{\infty}]$ used to be needed so that the Radon measures take finite values on the tail regions; that is, regions bounded away from $\{\mathbf{0}\}$. Such compactification poses problems with, for example, establishing equivalence of vague convergences under Cartesian coordinate and polar coordinate, since polar coordinate transformation such as $\boldsymbol{x} :\mapsto (\|\boldsymbol{x}\|, \boldsymbol{x}/\|\boldsymbol{x}\|)$, where $\|\boldsymbol{x}\|$ denotes a norm of $\boldsymbol{x}$, is only defined on $[\mathbf{0}, \boldsymbol{\infty}) \setminus \{\mathbf{0}\}$ and not on any lines through ∞. Compactification also makes geometric interpretations involving lines through ∞ confusing. The new definition through $\mathbb{M}$ convergence is given by measures that are finite on sets bounded away from $\{\mathbf{0}\}$. The finiteness of the measures on such sets removes the need for compactifying the space. Another advantage of the $\mathbb{M}$ convergence formulation is that MRV as described in ($\mathbf{C}_1$) enables the definition of regular variation on a space with a chosen forbidden zone excluded, thereby facilitating the definition of hidden regular variation on various types of spaces of interest (Das et al., 2013).

One may equip the space of $\mathbb{M}\left(\mathbb{R}_+^n \setminus \{\mathbf{0}\}\right)$ with a metrizable topology similar to the vague topology (Resnick, 2007, Section 3.3.5). For more discussions about the problems with the traditional MRV definition, the advantages of using $\mathbb{M}$ convergence, a choice of topology and metric for $\mathbb{M}\left(\mathbb{R}_+^n \setminus \{\mathbf{0}\}\right)$, etc., see Das et al. (2013), Lindskog et al. (2014), and Das and Resnick (2017).

In general, to establish $\mathbb{M}$ convergence in $\mathbb{M}(\mathbb{C} \setminus \mathbb{C}_0)$, an easy way is to show that the sequence $\{\mu_i\}_{i \geq 1}$ is relatively compact and that convergence holds on a class of convergence-determining sets, usually a π-system.

This is easier for the case of regular variation with $\mathbb{C} = \mathbb{R}_+^n$ or $\mathbb{R}^n$ and $\mathbb{C}_0 = \{\mathbf{0}\}$ since relative compactness of the sequence of measures is easier to establish. For example, for regular variation on $\mathbb{R}_+^n \setminus \{\mathbf{0}\}$, relative compactness of the sequence is implied when the convergence of the sequence to the limit measure holds on the determining class of sets that take the form of $A_{\boldsymbol{x}} = [\mathbf{0}, \boldsymbol{x}]^c$, $\boldsymbol{x} \in \mathbb{R}_+^n$. This means that $\mathbb{M}$ convergence in $\mathbb{M}\left(\mathbb{R}_+^n \setminus \{\mathbf{0}\}\right)$ can be demonstrated by proving convergence on all sets of $A_{\boldsymbol{x}}$ given above. Therefore, $\mathbb{M}$ convergence of $\{\mu_i\}_{i\geq 1}$ in $\mathbb{M}\left(\mathbb{R}_+^n \setminus \{\mathbf{0}\}\right)$ is equivalent to vague convergence of $\{\mu_i\}_{i\geq 1}$ in the space of nonnegative Radon measures on $[\mathbf{0}, \boldsymbol{\infty}]^n \setminus \{\mathbf{0}\}$, and hence, at least in the case with $\mathbb{C} = \mathbb{R}_+^n$ or $\mathbb{R}^n$ and $\mathbb{C}_0 = \{\mathbf{0}\}$, the switch from the traditional definition of MRV to the new one is seamless and many results established under vague convergence are still applicable. See, for example, Section 3.1 of Das et al. (2013) for related discussions.

A few comments on condition ($\mathbf{C}_1$) follow. Essentially, the condition is the same as Assumption 2.1 of Asimit et al. (2011), which implies asymptotic dependence among the risk RVs in $\boldsymbol{X}$. It is well known that it also implies $\boldsymbol{X}$ has equivalent tails that are regularly varying. That is, we have $X_i \in \mathrm{RV}_{-\alpha}$ for some $\alpha > 0$ and every $i \in \mathcal{N}$. Moreover,

$$\lim_{t\to\infty} \frac{\overline{F}_i(t)}{\overline{F}_1(t)} = \lim_{t\to\infty} \frac{P\left(X_i > t, \bigcap_{j\neq i}(X_j \geq 0)\right)}{\overline{F}_1(t)} = \mu(\mathbb{R}_+ \times \cdots \times (1,\infty) \times \mathbb{R}_+ \times \cdots \times \mathbb{R}_+) =: c_i, \tag{14}$$

where $c_i \in (0,\infty)$, $i \in \mathcal{N}$. Using similar reasoning, we can see that the nonnegativity of X_j's is not essential. In fact, the same conclusion would hold as long as there exists a real-valued lower bound for X_j's, which is not surprising given that we are modeling the right-tail behavior.

We use a bivariate case to illustrate the MRV assumption specified in ($\mathbf{C}_1$) in a more accessible manner.

Remark 4.1. *Consider a random pair (X_1, X_2) that satisfies the MRV assumption in (13) of ($\mathbf{C}_1$). Then the tails of the marginal distributions of both X_1 and X_2 satisfy the tail equivalence relationship specified in (14). Well-known univariate distribution models with regularly varying tails include the Pareto, Fréchet, Burr, and Lomax distributions. It is worth noting that the MRV assumption in ($\mathbf{C}_1$) does not require the marginal distributions of X_1 and X_2 to follow the same distribution family. Instead, it only requires that their marginal tails decay at the same rate. For instance, it is valid for X_1 following a Pareto distribution and X_2 following a Burr distribution with the same tail index.*

MRV constitutes a flexible and versatile framework for modeling dependence, as it can accommodate both tail dependence and tail independence. For many commonly used parametric copula models, as long as the accompanying marginal distributions satisfy the regular variation and tail equivalence assumptions described above, the resulting pair (X_1, X_2) falls within the MRV framework.

Theorem 4.2. *Suppose that the risk vector $\boldsymbol{X}$ satisfies condition ($\mathbf{C}_1$). Then the GTE-based proportional allocation*

in equation (5) satisfies

$$\lim_{q\uparrow 1}\tilde{r}_{i,q}=\int_0^1\frac{\mu(A_{i,z})}{\mu(\aleph)}\,dz,\qquad i\in\mathcal{N},\tag{15}$$

where $A_{i,z}=\left\{\boldsymbol{x}\in\mathbb{R}_+^n:x_i>z\sum_{k=1}^n x_k,\sum_{k=1}^n x_k>1\right\}$ *and* $\aleph=\left\{\boldsymbol{x}\in\mathbb{R}_+^n:\sum_{k=1}^n x_k>1\right\}$.

Proof. See Appendix A. □

In practical applications, it may be more convenient to work with an asymptotic result expressed in terms of the spectral measure rather than the limit measure. Next, we are going to rewrite our result in Theorem 4.2 via a semi-parametric form using the spectral measure. To this end, write $\boldsymbol{Y}=\left(1/\overline{F}_1(X_1),\ldots,1/\overline{F}_n(X_n)\right)$. Under the condition of Theorem 4.2, there exists a measure μ^*, such that, for any $x>0$,

$$t\,P\left(\bigcup_{i=1}^n(Y_i>x_it)\right)\to\mu^*[0,x]^c;$$

see, e.g., Proposition 5.10 of Resnick (2008). For some spectral measure H, which is a probability measure, on $\mathcal{W}_{n-1}=\left\{\boldsymbol{x}\in\mathbb{R}_+^n:\sum_{k=1}^n x_k=1\right\}$, the limit measure μ^* satisfies $\mathrm{d}\mu^*\circ T^{-1}=n\,r^{-2}\mathrm{d}r\times\mathrm{d}H$, where T maps $\boldsymbol{x}\in\mathbb{R}_+^n$ into $(r,\boldsymbol{w})=(\sum_{k=1}^n x_k,x/\sum_{k=1}^n x_k)\in(0,\infty)\times\mathcal{W}_{n-1}$, and T^{-1} denotes its inverse.

Proposition 4.3. *The asymptotic expression for the GTE-based proportional allocation in Theorem 4.2 can be rewritten in terms of a spectral measure H as follows:*

$$\lim_{q\uparrow 1}\tilde{r}_{i,q}=\frac{\int_{\mathcal{W}_{n-1}}c_i^{1/\alpha}w_i^{1/\alpha}\left(\sum_{k=1}^n c_k^{1/\alpha}w_k^{1/\alpha}\right)^{\alpha-1}H(\mathrm{d}w)}{\int_{\mathcal{W}_{n-1}}\left(\sum_{k=1}^n c_k^{1/\alpha}w_k^{1/\alpha}\right)^{\alpha}H(\mathrm{d}w)}.\tag{16}$$

Proof. See Appendix A. □

As the succeeding remark will show, despite the distinct expressions between the asymptotic results for the GTE-based allocation, given by (15) in this paper, and the CTE-based allocation, given by Theorem 2.1 of Asimit et al. (2011), a closer examination reveals that they are actually identical. However, an important difference is that the asymptotic result derived for the GTE-based allocation in this paper is applicable to infinite-mean models, whereas the CTE-based allocation in the literature is not. As noted earlier, infinite-mean models have attracted increasing scholarly attention in risk management, particularly in the contexts of climate risk, catastrophe risk, and operational risk (again, for a comprehensive review of recent research on infinite-mean models, we refer the reader to Chen and Wang, 2025). This suggests that the GTE-based allocation is a more versatile alternative to the CTE-based allocation widely studied in the existing literature.

Remark 4.4. *Under condition* ($\mathbf{C}_1$)*, Theorem 2.1 of Asimit et al. (2011), together with Proposition 7.3 of Resnick (2007) and equation (9) of Hua and Joe (2011a), implies that, if* $\alpha > 1$*, then*

$$\begin{aligned}\lim_{q\uparrow 1} r_{i,q} &= \frac{\alpha-1}{\alpha}\frac{\frac{1}{\alpha-1}\mu\left(\boldsymbol{x}\in\mathbb{R}_+^n : x_i>1\right)+\int_0^1 \mu\left(\boldsymbol{x}\in\mathbb{R}_+^n : x_i>z, \sum_{k=1}^n x_k>1\right)\mathrm{d}z}{\mu\left(\boldsymbol{x}\in\mathbb{R}_+^n : \sum_{k=1}^n x_k>1\right)}\\ &= \frac{c_i+(\alpha-1)\int_0^1 \mu\left(\boldsymbol{x}\in\mathbb{R}_+^n : x_i>z, \sum_{k=1}^n x_k>1\right)\mathrm{d}z}{\alpha\mu(\aleph)}, \qquad i\in\mathcal{N},\end{aligned}$$

where c_i *is given by equation* (14)*. By using a similar idea to that in the proof of Proposition 4.3 to convert the expression above using the sepctral measure, one can show that the right-hand side of the equation above can also be written as the expression in* (16)*, and hence,*

$$\lim_{q\uparrow 1} r_{i,q} = \lim_{q\uparrow 1} \tilde{r}_{i,q}, \qquad \textit{for all } i\in\mathcal{N}.$$

The seemingly surprising asymptotic identity above aligns well with our intuition. To see this, note that the decomposition of the limit measure under MRV into a product measure (see Theorem 6.1(4) of Resnick, 2007) shows that the radial component S *and the polar coordinate component* $\boldsymbol{X}/S$ *are independent in the tail. Consequently, for* S *sufficiently large, the conditional covariance between* S *and* R_i*, defined by equation* (6)*, diminishes. This implies that* $E(S\times R_i \,|\, S>s_q)$ *and* $E(S\,|\,S>s_q)\times E(R_i\,|\,S>s_q)$ *converge to the same value as* $q\uparrow 1$*, and hence so do* $r_{i,q}$ *and* $\tilde{r}_{i,q}$*.*

4.2 Gumbel case

In this section, we consider the case where the individual risks follow distributions that are in MDA(Λ). We shall assume the following condition:

($\mathbf{C}_2$) For some positive function $a(\cdot)$ such that $a(t)=o(t)$ and some nonzero and nondegenerate measure μ on $[-\infty,\infty)^n\setminus\{-\infty\}$, the nonnegative risk vector $\boldsymbol{X}$ satisfies that

$$\frac{P((\boldsymbol{X}-t\mathbf{1})/a(t)\in\cdot)}{\overline{F}_1(t)}\to\mu \qquad \text{in } \mathbb{M}([-\infty,\infty)^n\setminus\{-\infty\}), \tag{17}$$

where $\mathbf{1}$ a vector with all components equal to 1 and the limit measure μ satisfies $\mu(-\infty,\infty)>0$.

Condition ($\mathbf{C}_2$) implies that the tails of X_i, $i\in\mathcal{N}$, are equivalent; specifically, $\overline{F}_i(t)\sim c_i\overline{F}_1(t)$, $i\in\mathcal{N}$, with $c_i=\mu(\boldsymbol{x}:x_i>0)$. Moreover, we remark that, for the limit measure μ in condition ($\mathbf{C}_2$), $\mu\big([-\infty,\cdot]^c\big)$ and $\mu\big((\cdot,\infty]\big)$ are continuous functions on $(-\infty,\infty)$. To see this, it suffices to show that, for small $\delta>0$ and $\boldsymbol{u},\boldsymbol{v}\in\mathbb{R}^n$ such

that $0 < v_i - u_i < \delta$, $i \in \mathcal{N}$, $\mu((\boldsymbol{u},\boldsymbol{v}])$ can be made arbitrarily close to 0. This is obvious since, by equation (31), $\mu((\boldsymbol{u},\boldsymbol{v}]) \leq \sum_{i=1}^{n} (\mu(\boldsymbol{x} : x_i > u_i) - \mu(\boldsymbol{x} : x_i > v_i)) = \sum_{i=1}^{n} c_i \left(e^{-u_i} - e^{-v_i}\right)$, which goes to 0 as $\delta \to 0$.

The following proposition states that condition ($\mathbf{C}_2$) is equivalent to what is essentially needed in Section 2.2 of Asimit et al. (2011), where their assumption, as described in equation (2.11) of their paper, is formulated in terms of vague convergence. The equivalence hinges on the fact that the limit measure assigns zero mass to the lines through $\boldsymbol{\infty}$.

Proposition 4.5. *The $\mathbb{M}$ convergence given in condition ($\mathbf{C}_2$) is equivalent to the existence of some positive auxiliary function $a(\cdot)$ satisfying $a(t) = o(t)$ and some nonzero and nondegenerate Radon measure ν on $[-\infty,\infty]^n \setminus \{-\boldsymbol{\infty}\}$, such that*

$$\frac{P((\boldsymbol{X} - t\mathbf{1})/a(t) \in \cdot)}{\overline{F}_1(t)} \xrightarrow{v} \nu \qquad \text{in } \mathbb{M}_+\left([-\infty,\infty]^n \setminus \{-\boldsymbol{\infty}\}\right), \tag{18}$$

where $\mathbb{M}_+\left([-\infty,\infty]^n \setminus \{-\boldsymbol{\infty}\}\right)$ denotes the set of all nonnegative Radon measures on $[-\infty,\infty]^n \setminus \{-\boldsymbol{\infty}\}$.

Proof. See Appendix A. □

To demonstrate that Condition ($\mathbf{C}_2$) is satisfied by commonly used distributions and dependence structures, we present the following simple illustrative example:

Example 1. *Suppose that (U_1, U_2) is a vector of two uniform RVs on $[0,1]$ distributed by a Gumbel copula*

$$C(u_1,u_2) = \exp\left\{-\left((-\log u_1)^{\beta} + (-\log u_2)^{\beta}\right)^{1/\beta}\right\}, \qquad (u_1,u_2) \in [0,1]^2 \tag{19}$$

with $\beta > 1$. Also suppose that, for some $c > 0$,

$$\widetilde{U}_2 = \left(1 - \frac{1-U_2}{c}\right) 1_{(U_2 > 1-c)}.$$

Now, let $X_1 = F^{-1}(U_1)$ and $X_2 = F^{-1}(\widetilde{U}_2)$, where $F(x)$ is the cumulative distribution function of an exponential distribution with mean θ, and F^{-1} is its inverse function. It is easy to verify that X_1 follows an exponential distribution and that $\overline{F}_2(t) \sim c\overline{F}_1(t)$.

Moreover, for $a(\cdot) = \theta$ and for every $(x_1,x_2) \in \mathbb{R}^2$, it holds for t large that

$$P\left(\frac{\boldsymbol{X} - t\mathbf{1}}{a(t)} \in [-\boldsymbol{\infty},(x_1,x_2)]^c\right) = 1 - C\left(1 - \exp\left\{-\left(\frac{t}{\theta} + x_1\right)\right\}, 1 - \exp\left\{-\left(\frac{t}{\theta} + (x_2 - \ln c)\right)\right\}\right).$$

With some algebra, it follows that

$$\lim_{t\to\infty} \frac{P((\boldsymbol{X} - t\mathbf{1})/a(t) \in [-\boldsymbol{\infty},(x_1,x_2)]^c)}{\overline{F}_1(t)} = \left(e^{-x_1\beta} + c^{\beta} e^{-x_2\beta}\right)^{1/\beta}.$$

By Proposition 4.5, the convergence in equation (17) holds with limit measure μ given by

$$\mu\big([-\infty,\boldsymbol{x}]^c\big)=\Big(\mathrm{e}^{-x_1\beta}+c^{\beta}\mathrm{e}^{-x_2\beta}\Big)^{1/\beta},\qquad \boldsymbol{x}\in\mathbb{R}^2,$$

which obviously satisfies $\mu(-\infty,\infty)>0$. This verifies that the random vector (X_1,X_2) satisfies condition ($\mathbf{C}_2$).

In fact, we can verify condition ($\mathbf{C}_2$) for many other choices of copulas besides the Gumbel copula above, such as the survival Clayton copula and non-independent extreme-value copulas.

The equivalence given by Proposition 4.5 above and Note 2.2 of Asimit et al. (2011) allow us to conclude that, under condition ($\mathbf{C}_2$),

$$P(S>nt)\sim\mu\Big(\boldsymbol{x}:\sum_{k=1}^{n}x_k>0\Big)\,\overline{F}_1(t). \tag{20}$$

Theorem 4.6. *Suppose that risk portfolio $\boldsymbol{X}$ has joint distribution satisfying condition ($\mathbf{C}_2$). Then it holds that*

$$\lim_{q\uparrow 1}\tilde{r}_{i,q}=\frac{1}{n},\qquad i\in\mathcal{N}.$$

Proof. See Appendix A. □

Remark 4.7. *By Theorem 2.2 and equation (2.15) of Asimit et al. (2011), it is obvious that, under condition ($\mathbf{C}_2$), the CTE-based proportional allocation $r_{i,q}\to 1/n$ as $q\uparrow 1$, $i\in\mathcal{N}$, meaning that, asymptotically, it agrees with the GTE-based counterpart.*

5 Asymptotically independent portfolios

5.1 Fréchet case

The first Fréchet case we consider in this section follows a setup similar to that in Section 4.1, except that we now assume asymptotic independence. Naturally, this leads to a more transparent result regarding the limit of the GTE-based allocation.

($\mathbf{C}_3$) Suppose that the nonnegative risk vector $\boldsymbol{X}$ satisfies the $\mathbb{M}$ convergence in condition ($\mathbf{C}_1$) and that the limit measure $\mu=\mu_I$ which only assigns mass to the axes.

An illustrative bivariate example of condition ($\mathbf{C}_3$), in contrast to its tail dependence counterpart ($\mathbf{C}_1$), is provided below.

Remark 5.1. *Suppose that a random pair (X_1,X_2) satisfies condition ($\mathbf{C}_3$), then their marginal distributions possess the same properties as those described in Remark 4.1; namely, both marginals exhibit regularly varying tails with*

a common tail index. However, in this case, the dependence between X_1 and X_2 in the joint upper tail region is weaker in the sense that the probability limit specified in (12) equals zero.

It is noteworthy that under Condition ($\mathbf{C}_3$), the extremal co-movement between X_1 and X_2 may be still stronger than that under full independence. Specifically, let $C:[0,1]^2\to[0,1]$ be the copula function underlying (X_1,X_2). Recall that the intermediate upper tail dependence index is defined, when the limiting relationship exists, as (Hua and Joe, 2011b):

$$\overline{C}(u,u)\sim u^{\kappa}\ell(u),\qquad \text{as } u\downarrow 0,$$

where $\ell(\cdot)$ is a slowly varying function at zero (i.e., $\ell(1/\cdot)$ is regularly varying at ∞ with index 0), and $\overline{C}(u,v):=1-u-v+C(u,v)$, $u,v\in[0,1]$, is the survivor copula function governing the co-movement of X_1 and X_2 in the upper joint tail region. Condition ($\mathbf{C}_3$) implies that the underlying copula C satisfies $\kappa\geq 1$, whereas under complete independence, $\kappa=2$. In other words, although (X_1,X_2) is asymptotically independent, their joint upper tail probabilities may still decay more slowly than those of an independent pair. The Gaussian copula is a well-known example that exhibits such intermediate upper tail dependence.

Under condition ($\mathbf{C}_3$), equation (14) can be rewritten as

$$\lim_{t\to\infty}\frac{\overline{F}_i(t)}{\overline{F}_1(t)}=\mu_I\left(\mathbb{R}_+\times\cdots\times(1,\infty)\times\mathbb{R}_+\times\cdots\times\mathbb{R}_+\right)=\mu_I\left(\boldsymbol{x}:x_i>1,x_j=0\text{ for all }j\neq i\right)=:c_i\in[0,\infty).$$

Note that we also have $\mu_I\left(\boldsymbol{x}\in\mathbb{R}_+^n:x_i>z\right)=c_iz^{-\alpha}$ for $z>0$.

Theorem 5.2. *Suppose that risk portfolio $\boldsymbol{X}$ satisfies condition ($\mathbf{C}_3$). Then it holds that*

$$\lim_{q\uparrow 1}\tilde{r}_{i,q}=\frac{c_i}{\sum_{k=1}^n c_k},\qquad i\in\mathcal{N}. \tag{21}$$

Proof. See Appendix A. □

Remark 5.3. *Comparing Theorem 5.2 with Theorem 3.1 of Asimit et al. (2011) and equation (9) of Hua and Joe (2011a), we can conclude that, if condition ($\mathbf{C}_3$) holds with tail index $\alpha>1$, then $\lim_{q\uparrow}r_{i,q}=\lim_{q\uparrow 1}\tilde{r}_{i,q}$.*

We now present the result for another structure where the components of $\boldsymbol{X}$ are asymptotically independent and belong to MDA(Φ). Note that in this case the tail indices of the risks are not necessarily the same.

($\mathbf{C}_4$) Suppose that the nonnegative risk vector $\boldsymbol{X}$ has marginal distributions F_i with $\overline{F}_i\in\text{RV}_{-\alpha_i}$, $\alpha_i>0$. Also suppose that there exist some measurable, bounded regularly varying functions $h_i(\cdot):(0,\infty)\to(0,\infty)$, such that, for distinct $i,j\in\mathcal{N}$, the relation $P(X_j>t\,|\,X_i=x)\sim\overline{F}_j(t)\,h_i(x)$ holds uniformly for $x\in[0,\infty)$. In addition,

for $n \geq 3$, it is also assumed that for distinct $i, j, k \in \mathcal{N}$, $P(X_j > t, X_k > t \,|\, X_i = x) = o\left(\overline{F}_j(t) + \overline{F}_k(t)\right) h_i(x)$ holds uniformly for $x \in [0, \infty)$.

Condition ($\mathbf{C}_4$) essentially encapsulates a collection of assumptions made in Assumption 3.2 and Theorem 3.2 of Asimit et al. (2011). It implies asymptotic independence among the risk positions in $\boldsymbol{X}$. The versatility and application of the dependence structure outlined in condition ($\mathbf{C}_4$) have been discussed extensively in the literature. For example, using the results in (Asimit and Badescu, 2010; Li et al., 2010), one may verify that nonnegative regularly varying RVs with pairwise dependence characterized by the Ali-Mikhail-Haq copula, the Farlie-Gumbel-Morgenstern, or the Frank copula—except for certain specific choices of parameters—all satisfy condition ($\mathbf{C}_4$).

Under condition ($\mathbf{C}_4$), it can be shown that, for $i \in \mathcal{N}$,

$$P\left(\sum_{k=1, k\neq i}^{n} X_k > t \,\middle|\, X_i = x\right) \sim h_i(x) \sum_{k=1, k\neq i}^{n} \overline{F}_k(t) \tag{22}$$

holds uniformly for $x \in [0, \infty)$. In addition, we have

$$P(S > t) \sim \sum_{k=1}^{n} \overline{F}_k(t), \tag{23}$$

indicating S has a regularly varying tail with index $\min_{1\leq i\leq n} \alpha_i$. See Lemma 3.2 and equation (3.12) in Theorem 3.2 of Asimit et al. (2011).

The following theorem contains our finding on the GTE-based allocation under condition ($\mathbf{C}_4$). It's worth noting that the result is formulated in terms of the ratio of tail distribution functions to accommodate various scenarios, with all tails being equivalent or with some dominating others.

Theorem 5.4. *Under condition ($\mathbf{C}_4$), it holds that*

$$\lim_{q\uparrow 1} \tilde{r}_{i,q} = \lim_{t\to\infty} \frac{\overline{F}_i(t)}{\sum_{k=1}^{n} \overline{F}_k(t)}, \qquad i \in \mathcal{N}, \tag{24}$$

provided that the limit on the right-hand side exists.

Proof. See Appendix A. □

Remark 5.5. *If the limit on right-hand side of (24) exists, then one may show that it agrees asymptotically with the corresponding CTE-based allocation when condition ($\mathbf{C}_4$) holds with $\alpha := \min_{1\leq i\leq n} \alpha_i > 1$. To see this, suppose that $\lim_{t\to\infty} \overline{F}_i(t) / \sum_{k=1}^{n} \overline{F}_k(t) = r \in [0, 1)$, and note that the CTE-based allocation satisfies*

$$\lim_{q\uparrow 1} r_{i,q} = \lim_{t\to\infty} \frac{E\left(X_i h_i\left(X_i\right)\right) \sum_{k=1, k\neq i}^{n} \overline{F}_k(t) + t\overline{F}_i(t) \frac{\alpha_i}{\alpha_i - 1}}{\sum_{k=1}^{n} \overline{F}_k(t)\, E(S|S > t)}$$

$$= \lim_{t\to\infty} \frac{\alpha-1}{\alpha} \frac{E\left(X_i h_i\left(X_i\right)\right) \sum_{k=1,k\neq i}^{n} \overline{F}_k(t) + t\overline{F}_i(t) \frac{\alpha_i}{\alpha_i - 1}}{t\sum_{k=1}^{n} \overline{F}_k(t)}$$
$$= \lim_{t\to\infty} \frac{\alpha-1}{\alpha} \frac{\alpha_i}{\alpha_i - 1} \frac{\overline{F}_i(t)}{\sum_{k=1}^{n} \overline{F}_k(t)}, \qquad i \in \mathcal{N}.$$

Noticing that $\alpha = \alpha_i$ for $r > 0$, we conclude that, for every $r \in [0,1)$, the above reduces to r, which is also the limit of the GTE-based allocation.

5.2 Gumbel case

Finally, in this subsection, we consider the case where the marginal distributions of $\boldsymbol{X}$ are in MDA(Λ) and the components are asymptotically independent. Specifically, motivated by Assumption 3.3 of Asimit et al. (2011) (see also Mitra and Resnick, 2009, Section 2.2), we introduce the following condition:[1]

($\mathbf{C}_5$) Suppose that the nonnegative risk vector $\boldsymbol{X}$ has marginal distribution $F_1 \in$ MDA(Λ) with $\overline{F}_i(t)/\overline{F}_1(t) \to c_i$ for some $c_i \in [0,\infty)$, $i \in \mathcal{N}$, and that $\overline{F}_1$ has auxiliary function $a(\cdot)$. Also suppose that, for every $x > 0$ and distinct $i, j \in \mathcal{N}$, it holds for some $L_{ij} > 0$ that

$$P\left(X_i > t, X_j > a(t)x\right) = o\left(\overline{F}_1(t)\right) \qquad \text{and} \qquad P\left(X_i > L_{ij}\,a(t), X_j > L_{ij}\,a(t)\right) = o\left(\overline{F}_1(t)\right). \tag{25}$$

Many practically useful distributions with asymptotic independence and marginal distributions in MDA(Λ) satisfy this condition. Examples of such distributions are provided and extensively discussed by (Mitra and Resnick, 2009, Section 3).

Theorem 5.6. *Under condition ($\mathbf{C}_5$), it holds that*

$$\lim_{q\uparrow 1} \tilde{r}_{i,q} = \frac{c_i}{\sum_{k=1}^{n} c_k}, \qquad i \in \mathcal{N}.$$

Proof. See Appendix A. □

Remark 5.7. *With Theorem 5.6, we can conclude that, by Theorem 3.3 and equation (2.15) of Asimit et al. (2011), the CTE-based and GTE-based allocations agree asymptotically when the risks in $\boldsymbol{X}$ belong to* MDA(Λ) *and satisfy the asymptotic independence condition in ($\mathbf{C}_5$).*

[1] Equation (3.24) in Asimit et al. (2011) contains a minor typo, making it a weaker condition compared to equation (25) included in condition ($\mathbf{C}_5$) of this current paper. However, the assumption used by Asimit et al. (2011) to obtain the desired asymptotics for the CTE-based allocation is exactly equation (25).

6 Numerical experiments

The numerical study in this section carries two main purposes. Firstly, it illustrates the desirable similarity between the CTE-based allocation and GTE-based allocation when the confidence level q is sufficiently close to 1. Secondly, it demonstrates the smaller variance of the empirical GTE allocation estimator compared to the one associated with the CTE-based allocation under some data scenarios, advocating for the adoption of the GTE-based allocation from a statistical robustness perspective.

6.1 An illustrative example

The set-up in this subsection is motivated by the simulation in Asimit et al. (2011). Specifically, we consider a portfolio comprising two dependent risks, denoted as $(X_1, X_2) \in \mathcal{X}^2$. The marginal distributions of X_1 and X_2 follow the Pareto distribution of the second kind (a.k.a., Lomax distribution), with survivial functions:

$$\overline{F}_i(x) = (1 + x/\lambda_i)^{-\alpha} \qquad \text{for } x > 0 \text{ and } i = 1, 2, \tag{26}$$

where $\lambda_i > 0$ and $\alpha > 0$ denote the scale and shape parameters, respectively. The distribution function in (26) belongs to the MDA of the Fréchet distribution. The distribution function $\overline{F}_i$ is regularly varying with a tail index α. The smaller the value of α, the heavier the tails of X_1 and X_2.

Further, the dependence between X_1 and X_2 is assumed to be governed by the Gumbel copula, specified in equation (19). Figure 2 illustrates the contour plot of the density of the Gumbel copula. As depicted, the Gumbel copula exhibits a positive dependence relationship in the upper tail region, with the strength of dependence increasing as β increases. The Gumbel copula combined with the marginal distributions in (26) implies that the joint distribution of (X_1, X_2) satisfies condition ($\mathbf{C}_1$).

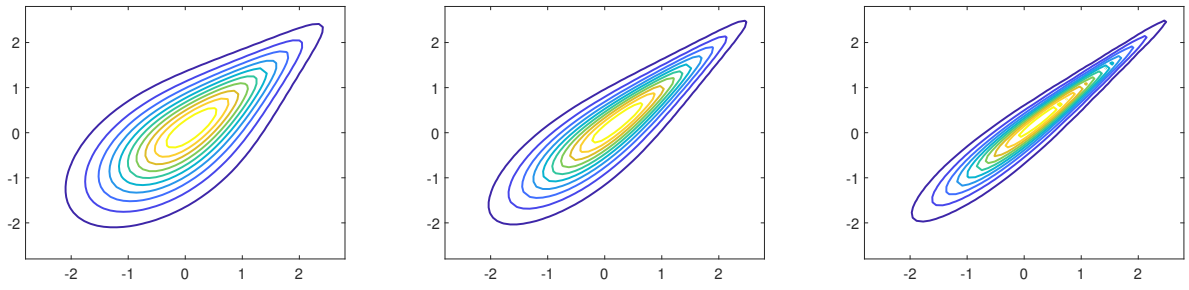

Figure 2: Contour plots of the density function of the Gumbel copula with standard normal margins for $\beta = 2$ in the left panel, $\beta = 3$ in the middle panel, and $\beta = 5$ in the right panel.

It is noteworthy that the dependence structure between X_1 and X_2, described by (19), is exchangeable. Namely,

$C(F_1(x_1),F_2(x_2)) = C(F_2(x_2),F_1(x_1))$, for all $x_1,x_2 > 0$. Thereby, if the scale parameters $\lambda_1 = \lambda_2$, then the joint distribution of (X_1,X_2) is exchangeable. In this case, the CTE-based allocation and GTE-based allocations are always identical for any confidence level $q \in [0,1)$, both equal to one half. For this reason, we generally assume $\lambda_1 \neq \lambda_2$ in order to highlight the asymptotic identify between the CTE-based and GTE-based allocations established in this current paper. The calculation of their limits is detailed in Appendix B.

Inspired by the simulation setup in Asimit et al. (2011), we assume the following parameter values in the baseline scenario:

- The tail index of the marginal distributions: $\alpha = 2$;
- The scale parameters of the marginal distributions: $\lambda_1 = 100\,000$ and $\lambda_2 = 300\,000$;
- The dependence parameter of the Gumbel copula: $\beta = 3$.

For each confidence level $q \in \{0.1, 0.5, 0.8, 0.95\}$, we simulate 10 000 pairs of X_1 and X_2 according to the joint distribution determined by (19) and (26). The empirical tail conditional expectation estimator proposed in Gribkova et al. (2022b) is used to estimate the corresponding CTE-based allocation $r_{i,q}$ and GTE-based allocation $\tilde{r}_{i,q}$, $i = 1,2$. This simulation exercise is repeated 500 times to construct the box plots of the allocation estimates, which are displayed in Figure 3. Note that the adopted tail conditional expectation estimator is already known to be consistent (Gribkova et al., 2022b), so the middle lines in the boxes can be viewed as numeric proxies for the true value of the allocation ratios, while the width of the boxes can be used to assess the robustness of the estimators.

As can be observed, when the confidence level is low (e.g., $q = 0.1$ and $q = 0.5$), the CTE-based and GTE-based allocations differ significantly. At the low confidence level of $q = 0.1$, the black dots are on the boundary or outside the whiskers of the $r_{i,q}$ and $\tilde{r}_{i,q}$ estimates, indicating that the limit provides a poor approximation of the true values of the two allocation ratios. As the confidence level increases to 0.5, the intervals associated with the two allocation methods move closer to the black dots. However, the allocation limit remains outside the whiskers of the GTE-based allocation $\tilde{r}_{i,q}$ estimates. As the confidence level q approaches 1, the medians of the CTE-based and GTE-based allocation estimates converge. At higher confidence levels (i.e., $q = 0.8$ and $q = 0.95$), the allocation limit dots fall within the middle region of the boxes, with the medians approximately matching the allocation ratio limit. Moreover, the intervals associated with the GTE-based allocation estimates are significantly narrower than those of the CTE-based allocation, suggesting that the GTE-based allocation is a statistically robust alternative to the CTE-based allocation when the confidence level is reasonably high.

It is noteworthy that although our paper focuses on asymptotic analysis, we intentionally include small values of q into this numerical experiment to illuminate that the differences between the CTE-based and GTE-based allocations can be substantial when q is small. Nevertheless, the differences diminish rapidly as q increases, and

the estimates from both allocation rules converge to the established limit rather quickly, particularly for the GTE-based allocation. This a welcoming finding, as it suggests that the limiting result established in the paper can provide a satisfactory approximation for both rules even when the confidence level q is moderately high, at least under the distributional settings given in (19) and (26).

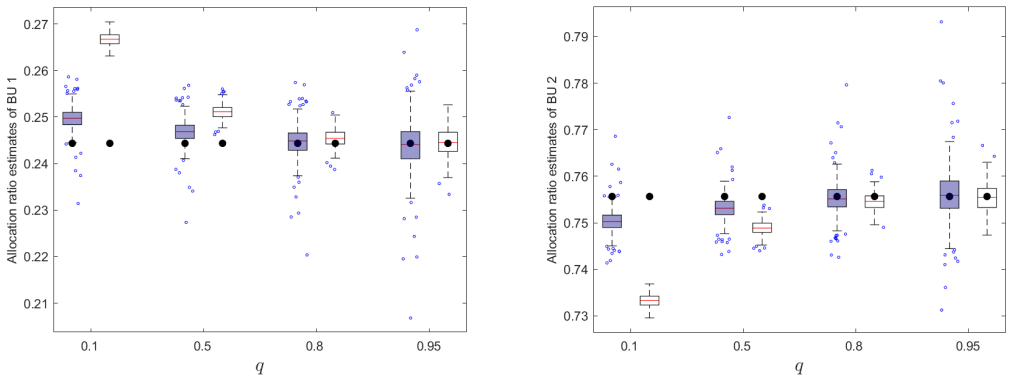

Figure 3: Box plots of the CTE-based allocation estimates (filled boxes) and GTE-based allocation estimates (blank boxes) at varying confidence levels. The black dots represent the limits of the two allocation methods, which are identical for the two allocation principles.

Next, we proceed by varying the tail parameter α and the copula dependence parameter β to study their impacts on our numerical findings. Since the allocation ratio for the second BU is one minus that for the first BU, in the following sensitivity analysis we report the results for the first BU only. Let us define the asymptotic approximation error as the difference between the limit of the CTE-based or GTE-based allocation and the mean of the corresponding allocation estimates. More formally, suppose that for a given sample size, the same simulation exercise is repeated m times. Then, the asymptotic approximation error is computed as

$$\left| \lim_{q \uparrow 1} \square_q - \frac{1}{m} \sum_{l=1}^{m} \widehat{\square}_{q,l} \right|, \tag{27}$$

where "$\square$" refers to either the CTE-based allocation r and the GTE-based allocation $\tilde{r}$, and "$\square_{q,l}$" denotes the corresponding estimate obtained by applying the empirical estimator from Gribkova et al. (2022b) to the data generated in the l-th simulation trial, for $l = 1, \ldots, m$. We set $m = 500$. Table 1 presents the aforementioned asymptotic approximation error for different values of tail parameter $\alpha \in \{0.8, 2, 3\}$. As mentioned earlier, the empirical estimator used is consistent (Gribkova et al., 2022a,b), so the means can be viewed as reasonable proxies for the true values of the corresponding CTE-based and GTE-based allocations.

We observe the following. Firstly, when $\alpha = 0.8$, the CTE-based allocation does not exist, let alone its limit. In contrast, the GTE-based allocation is always well-defined, and its limit exists. For all values of α considered, the

differences between the limits and the (mean approximated) true values become smaller as the confidence level q increases to 1. Secondly, focusing on the high confidence level case (i.e., $q = 0.95$), we find that the difference with the asymptotic approximation for $\alpha = 0.8$ and $\alpha = 2$ is smaller when $\alpha = 2$. This occurs because the magnitudes of the allocation ratios are larger when $\alpha = 0.8$. However, this pattern should not be interpreted as an indication that the asymptotic approximation performs better for risk portfolios with lighter tails. In fact, if we compare the asymptotic approximation difference between $\alpha = 2$ and $\alpha = 3$, where the magnitudes of the allocation ratios are close, we observe the opposite.

	$\alpha = 0.8$		$\alpha = 2$ (Baseline)		$\alpha = 3$	
	CTE method	GTE method	CTE method	GTE method	CTE method	GTE method
Limit	NA	25.60%	24.43%		24.49%	
$q = 0.1$	NA	2.14%	0.54%	2.24%	0.47%	1.99%
$q = 0.5$	NA	0.84%	0.25%	0.68%	0.12%	0.42%
$q = 0.8$	NA	0.30%	0.04%	0.12%	0.10%	0.06%
$q = 0.95$	NA	0.11%	0.03%	0.02%	0.12%	0.09%

Table 1: Summary of the asymptotic approximation errors, defined as the difference between the limit of the CTE-based or GTE-based allocation and the mean of the corresponding allocation estimates, for varying values of the tail parameter $\alpha \in \{0.8, 2, 3\}$. The row entiled "Limit" reports the limiting values of the CTE-based and GTE-based allocations, computed based on Theorem 4.2.

Table 2 presents the coefficients of variation (CVs) for the CTE-based and GTE-based allocation estimates under the same sensitivity analysis settings. Within the context of this numerical section, the CV of an allocation estimator is calculated as

$$\frac{(m-1)^{-1/2}\sqrt{\sum_{l=1}^{m}\left(\widehat{\square}_{q,l} - \sum_{l=1}^{m}\widehat{\square}_{q,l}/m\right)^2}}{\sum_{l=1}^{m}\widehat{\square}_{q,l}/m},$$

where "$\square_{q,l}$", $l = 1, \ldots, m$, are defined in the same way as in equation (27). As shown, across all tail parameter scenarios considered, the CV increases as the confidence level q grows, which is expected as fewer effective samples are used to estimate the allocation ratios. When comparing the CTE and GTE methods, the CV is consistently smaller for the empirical GTE-based allocation, except for the case of $q = 0.1$ and $\alpha = 3$, where they are comparable. In high confidence level and heavy-tailed scenarios (e.g., $q = 0.95$ and $\alpha = 0.8$ or 2), which are statistically challenging yet often encountered in practice, the CV associated with the GTE-based allocation estimator is significantly smaller than that of the CTE-based allocation. As a side note, it is worth mentioning that the conditional second moment of X_i given $S > s_q$ is not finite for $\alpha \in (0, 2]$. This explains the excessive volatilities associated with the empirical CTE-based allocation when α is low. The above discussion highlights the advantage of adopting the GTE-based allocation from a statistical robustness perspective.

	$\alpha = 0.8$		$\alpha = 2$ (Baseline)		$\alpha = 3$	
	CTE method	GTE method	CTE method	GTE method	CTE method	GTE method
Limit	NA	25.60%	24.43%		24.49%	
$q = 0.1$	28.74%	0.64%	0.97%	0.54%	0.50%	0.52%
$q = 0.5$	28.84%	0.83%	1.07%	0.59%	0.55%	0.54%
$q = 0.8$	29.13%	1.32%	1.37%	0.78%	0.72%	0.68%
$q = 0.95$	29.88%	2.73%	2.23%	1.37%	1.19%	1.08%

Table 2: Summary of the CVs for the CTE-based and GTE-based allocation estimators for the first BU, with varying tail parameters $\alpha \in \{0.8, 2, 3\}$. The row entiled "Limit" reports the limiting values of the CTE-based and GTE-based allocations, computed based on Theorem 4.2.

A similar sensitivity analysis is conducted for the Gumbel copula's dependence parameter β. According to the limit of allocation ratio shown in Table 3, a smaller value of β, or equivalently, corresponding to a weaker tail dependence, decreases the asymptotic risk allocation to the first BU. Comparing the cases of $\beta = 2$ and $\beta = 3$, the asymptotic approximation error is consistently larger for any considered q when $\beta = 2$, despite the higher corresponding allocation ratio. Although the error is higher when $\beta = 5$ compared to $\beta = 3$, this pattern is likely due to a larger allocation ratio to the BU under $\beta = 5$. Overall, these discussions suggest that a larger value of the dependence parameter β, or, a stronger tail dependence, may improve the performance of the asymptotic approximation.

	$\beta = 2$		$\beta = 3$ (Baseline)		$\beta = 5$	
	CTE method	GTE method	CTE method	GTE method	CTE method	GTE method
Limit	23.48%		24.43%		24.82%	
$q = 0.1$	6.24%	20.19%	0.54%	2.24%	0.67%	3.38%
$q = 0.5$	3.68%	8.52%	0.25%	0.68%	0.26%	0.78%
$q = 0.8$	1.12%	2.43%	0.04%	0.12%	0.02%	0.14%
$q = 0.95$	0.10%	0.22%	0.03%	0.02%	0.04%	0.16%

Table 3: Summary of the asymptotic approximation errors, defined as the difference between the limit of the CTE-based or GTE-based allocation and the mean of the allocation estimates, for varying values of the Gumbel copula's dependence parameter $\beta \in \{2, 3, 5\}$. The row entiled "Limit" reports the limiting values of the CTE-based and GTE-based allocations, computed based on Theorem 4.2.

Table 4 summarizes the changes in the CV for allocation estimates in response to varying values of β. The results indicate that the GTE-based allocation estimator consistently outperforms the CTE-based one, exhibiting lower variation across all dependence scenarios considered. With a fixed confidence level, a larger value of β, corresponding to stronger dependence in the copula, enhances the robustness of both the CTE-based and GTE-

based allocation estimators.

	$\beta = 2$		$\beta = 3$ (Baseline)		$\beta = 4$	
	CTE method	GTE method	CTE method	GTE method	CTE method	GTE method
Limit	23.48%		24.43%		24.82%	
$q = 0.1$	1.54%	0.72%	0.97%	0.54%	0.57%	0.35%
$q = 0.5$	1.72%	0.88%	1.07%	0.59%	0.62%	0.35%
$q = 0.8$	2.27%	1.27%	1.37%	0.78%	0.79%	0.45%
$q = 0.95$	3.76%	2.30%	2.23%	1.37%	1.27%	0.77%

Table 4: Summary of the CVs for the CTE-based and GTE-based allocation estimators for the first BU, with varying tail parameters $\beta \in \{2, 3, 5\}$. All values are reported in the unit of percentage. The row entiled "Limit" reports the limiting values of the CTE-based and GTE-based allocations, computed based on Theorem 4.2.

Collectively, we observe that in this particular simulation example, the empirical GTE-based allocation may outperform the empirical CTE-based allocation in terms of smaller variance in the presence of heavy tails and strong tail dependence. An intuition for this observation is that this distributional scenario implies more frequently occurring extreme values in X_i and S, which tend to occur simultaneously due to strong tail dependence. By taking the conditional mean of the ratio as in the GTE-based allocation, the presence of extremes in X_i and S is directly captured and balanced out, stabilizing the individual ratios and reducing the variance of the estimator. In contrast, the ratio of conditional means, as in the CTE-based allocation, first averages X_i and S separately. These averages tend to smooth out the extreme values to some extent, but the corresponding balancing effect is less efficient compared to directly taking the ratio at the individual level. We openly admit that this observation about the smaller variance associated with the empirical GTE-based allocation is based on a single simulation example. In the following subsection, we will conduct a robustness check of the aforementioned numerical observation by varying the marginal distributions and the underlying copula of (X_1, X_2).

6.2 Robustness check

Since the asymptotic equivalence between the CTE-based and GTE-based allocations has already been established theoretically, this subsection focuses on the numerical comparison of the statistical robustness of the empirical estimators associated with these two allocation rules across a broader set of distributional settings.

We first vary the marginal distributions by considering the following set of models:

- Fréchet distribution: $\overline{F}_i(x) = 1 - \exp\{-(x/\lambda_i)^{-\alpha}\}, \quad x > 0$;
- Paralogistic distribution: $\overline{F}_i(x) = (1 + (x/\lambda_i)^{\sqrt{\alpha}})^{-\sqrt{\alpha}}, \quad x > 0$;
- Inverse-Gamma distribution: $\lambda_i / X_i \sim \text{Gamma}(\alpha, 1), \quad i = 1, 2.$

For the sake of consistency across all alternative models, we set $\alpha = 2$, $\lambda_1 = 100\,000$, $\lambda_2 = 300\,000$, which ensures that their tail indices and tail ratios match those of the baseline case considered in Section 6.1. The copula function governing the dependence of (X_1, X_2) remains the same as in the setup of Section 6.1, namely the Gumbel copula with dependence parameter $\beta = 3$.

The CVs of the empirical estimator for the CTE-based allocation and the GTE-based allocation under varying marginal distributions are summarized in Table 5. As observed, the GTE-based method consistently yields lower CVs across all marginal distribution choices, which indicate a clear advantage in statistical robustness over the CTE-based method. This advantage is especially pronounced under Fréchet and Paralogistic marginals, but remains noticeably present in the Inverse-Gamma case.

	Fréchet		Paralogistic		Inverse-Gamma	
	CTE method	GTE method	CTE method	GTE method	CTE method	GTE method
$q = 0.1$	0.60%	0.24%	0.74%	0.43%	0.59%	0.29%
$q = 0.5$	0.76%	0.34%	0.84%	0.49%	0.72%	0.41%
$q = 0.8$	1.14%	0.59%	1.15%	0.66%	1.02%	0.64%
$q = 0.95$	2.06%	1.17%	2.02%	1.25%	1.78%	1.22%

Table 5: Summary of the CVs for the CTE-based and GTE-based allocation estimators for the first BU, under Fréchet, Paralogistic, and Inverse-Gamma marginals.

Next, we keep the marginal distributions as the Lomax distribution specified in (26), but vary the dependence structure of (X_1, X_2). Specifically, we consider a set of alternative copula models that, like the Gumbel copula examined in the previous subsection, exhibit upper tail dependence. These models include, for $(u_1, u_2) \in [0,1]^2$,

- Survival Clayton copula: $C(u_1, u_2) = u_1 + u_2 - 1 + [(1-u_1)^{-\theta} + (1-u_2)^{-\theta} - 1]^{-1/\theta}$, $\theta > 0$;
- Joe copula: $C(u_1, u_2) = 1 - \left[(1-u_1)^{\theta} + (1-u_2)^{\theta} - (1-u_1)^{\theta}(1-u_2)^{\theta}\right]^{1/\theta}$, $\theta > 1$;
- Student's t copula: $C(u_1, u_2) = T_{\nu,\rho}\left(T_{\nu}^{-1}(u_1), T_{\nu}^{-1}(u_2)\right)$, where $T_{\nu,\rho}(\cdot,\cdot)$ denotes the bivariate t distribution function with degree of freedom $\nu > 0$ and correlation parameter $\rho \in (-1, 1)$, and $T_{\nu}(\cdot)$ is the univaraite t distribution function.

To facilitate a meaningful comparison, in the succeeding numerical experiment, we calibrate the parameters of the aforementioned alternative copula models to match the dependence structure of the Gumbel copula considered earlier. Specifically, for the one-parameter copula models, we choose their parameters so that the corresponding upper tail dependence coefficient: $\lambda := \lim_{u \uparrow 1} [1 - 2u + C(u,u)]/(1-u)$, matches that implied by the Gumbel copula considered in Section 6.1 with baseline dependence parameter $\beta = 3$. For the Student's t copula, which involves two parameters, we additionally match its Kendall's tau to that of the Gumbel copula to determine a consistent parameter choice. The values of parameters specified to the alternative copula models are summarized in Table 6.

Copula model	Parameter choice
Survival Clayton copula	$\theta = 2.303$
Joe copula	$\theta = 3$
Student's t copula	$\nu = 1.014$ $\rho = 0.866$

Table 6: Summary of the parameter values chosen for the alternative copula models used in the robustness check.

The CVs for the CTE-based and GTE-based allocation estimators under the three alternative copula models outlined above are summarized in Table 7. As observed, across all confidence levels and copula models considered, the GTE-based allocation estimator consistently demonstrates greater statistical robustness in terms of lower CV values compared to the CTE-based estimator. Collectively, these results support the favorable use of the GTE-based method as a robust alternative to the CTE-based approach in the presence of heavy-tailed margins and strong tail dependence.

	Survival Clayton		Joe		Student's t	
	CTE method	GTE method	CTE method	GTE method	CTE method	GTE method
$q = 0.1$	0.95%	0.66%	0.94%	0.69%	1.18%	0.55%
$q = 0.5$	1.06%	0.72%	1.04%	0.77%	1.31%	0.75%
$q = 0.8$	1.36%	0.89%	1.32%	0.84%	1.74%	1.11%
$q = 0.95$	2.18%	1.48%	2.14%	1.36%	2.88%	1.96%

Table 7: Summary of the CVs for the CTE-based and GTE-based allocation estimators for the first BU, under Survival Clayton, Joe, and Student's t copulas.

7 Real-data demonstration

In this section, we demonstrate that the desirable asymptotic parity between the CTE-based and GTE-based allocations, as well as the greater statistical robustness the GTE-based method, continue to hold in real data, which is noisier and where the tail assumptions may be less perfectly satisfied than in the idealized simulation setting.

Our real-data illustration is based on the Danish fire losses dataset (McNeil, 1997). The data contains 2 156 entries of large fire claims in Denmark, spanning from January 1980 to December 1990. Each entry has three dimensions, representing inflation-adjusted losses attributed to building, content, and profit coverages, denoted by X_1, X_2, and X_3, respectively. We aim to assess the risk contribution of each individual coverage to the total loss using both the CTE-based and GTE-based allocation methods.

The literature has reported that both the marginal distributions and the aggregate distribution of the losses in the Danish fire losses dataset exhibit heavy-tailed behavior (Lehtomaa and Resnick, 2020; McNeil, 1997; Resnick,

1997). Inspection of the Hill plots for each marginal distribution reveals that the estimated tail indices fluctuate between 1 and 2, which is broadly consistent with the related results reported in the literature (Lehtomaa and Resnick, 2020; McNeil, 1997; Resnick, 1997). Recall that MRV, as specified in condition ($\mathbf{C}_1$), makes up a comprehensive framework for capturing a broad range of extremal dependence, as long as the marginal distributions satisfy the regular variation and tail equivalence assumptions. Given the similarity in tail index estimates across the marginal distributions of $\boldsymbol{X} = (X_1, X_2, X_3)$, we argue that it is reasonable to model $\boldsymbol{X}$ using MRV.

We are well aware of the sensitivity of Hill's estimator to the choice of tuning parameter which determines the number of upper order statistics included in the estimation process. This sensitivity, compounded by the typically wide confidence intervals of the tail indices, especially when a high threshold is chosen, makes it challenging to conclusively determine whether the margins are truly tail equivalent. To further assess the reasonableness of modeling $\boldsymbol{X}$ under the MRV framework, we applied the hypothesis testing procedure proposed by Einmahl et al. (2021). Their proposed test statistic is given by

$$T_n = \frac{k}{m} \sum_{j=1}^{m_1} \sum_{l=1}^{m_2} \left(\frac{\hat{\gamma}_{j,l}}{\hat{\gamma}_{\text{all}}} - 1 \right)^2,$$

where $k \in \mathbb{N}$ is a tuning parameter that determines the number of largest radii from the polar transformation of $\boldsymbol{X}$, to be included in the estimation. The parameters $m_1, m_2 \in \mathbb{N}$ specify how the joint region, formed by the radii and one angular component of the polar-transformed data, is partitioned into $m = m_1 \times m_2$ blocks. Following the recommendation in Einmahl et al. (2021), we set $m_1 = m_2 = 2$ in our analysis. Within each block, the Hill estimate of the tail index of the radii is denoted by $\hat{\gamma}_{j,l}$ for $j = 1, \ldots, m_1$ and $l = 1, \ldots, m_2$. The overall Hill estimate based on all radii exceeding the k-th order statistic is denoted by $\hat{\gamma}_{\text{all}}$. Under certain regularity conditions, the asymptotic distribution of T_n follows a chi-square distribution with $(m-1)$ degrees of freedom.

In a similar vein to many tail-related statistical methods, the aforementioned testing procedure for MRV requires the specification of tail regions, which raises a certain degree of subjectivity. Admittedly, the test results can be quite sensitive to the choice of the threshold parameter k. To mitigate this subjectivity, it is commonly advised to perform the test under multiple values of k. Figure 4 reports the p-values of the MRV test across a range of threshold values. As shown, the p-values fluctuate noticeably depending on the choice of k. For most sufficiently small values of k considered, the null hypothesis that $\boldsymbol{X}$ follows an MRV structure cannot be rejected at the 10% significance level or lower. Moreover, the p-values exhibit a generally increasing trend as the threshold parameter k decreases, suggesting that as the testing shifts deeper into the tail region, it becomes increasingly difficult to reject the MRV assumption. Thereby, we conclude that modeling the tail of $\boldsymbol{X}$ under the MRV framework is reasonable.

Nevertheless, we openly acknowledge that no statistical assumption can be expected to hold perfectly for real-

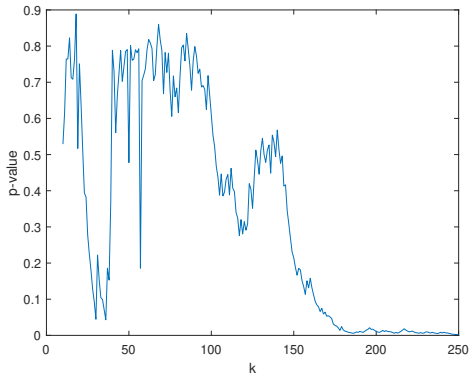

Figure 4: Summary of the p-value of the MRV test calculated under varying values of threshold parameter k.

world data, and the MRV framework is no exception. In what follows, we illustrate that despite potential model misspecification, the allocation limit derived in Theorem 4.2 correctly captures the trend toward which the empirical estimates converge as the confidence level q increases to 1. To compute the limit in (15), we resort to its spectral measure representation reported in Proposition 4.3, and apply the empirical method considered in Qin and Zhou (2021) to estimate it.

Recall that the Hill estimates of the tail indices across different margins range between 1 and 2. Accordingly, we assume that the common tail index α in the MRV framework falls within this range. For a given estimate of the common tail index $\hat{\alpha} \in (1,2)$, we estimate the tail equivalence ratios by first determining the threshold for upper order statistics along each margin, denoted by $\hat{k}_i$, $i = 1,2,3$, such that the implied Hill estimate matches the common tail index assumed. The tail equivalence ratio is then estimated via $\hat{c}_i = \hat{a}_i/\hat{a}_1$, with $\hat{a}_i = \left[\left(X_{i,(N-\hat{k}_i)}\right)^{\hat{\alpha}} \hat{k}_i\right]/N$, where N is the total sample size, and $X_{i,(1)} \leq X_{i,(2)} \leq \cdots \leq X_{i,(N)}$ denote the order statistics of $X_{i,1},\ldots,X_{i,N}$, which are independent samples of X_i, $i = 1,2,3$.

Next, we turn to estimating the spectral measure H on $\mathcal{W}_{n-1}$, where in this example, the dimension $n = 3$. For a fixed $i \in \{1,2,3\}$, $\text{rank}(X_{i,j})$ represents the rank of the j-th sample of X_i, ordered from smallest to largest. Moreover, define

$$z_j = \sum_{i=1}^{3} \frac{N+1}{N+1-\text{rank}(X_{i,j})}, \qquad j = 1,\ldots,N.$$

Let $\mathcal{S} = \{j : \text{rank}(z_j) \geq N+1-b\}$ collect the indices of samples considered as tail observations, as defined by a properly chosen parameter $b \in \mathbb{N}$. In this analysis, we set $b = 40$, corresponding to approximately the top $(b/N \times 100)\% \approx 2\%$ of the data. For each $j \in \mathcal{S}$, the point

$$\left(\frac{N+1-\text{rank}(X_{1,j})}{z_j}, \frac{N+1-\text{rank}(X_{2,j})}{z_j}, \frac{N+1-\text{rank}(X_{3,j})}{z_j}\right)$$

represents the intersection between the plane $\mathcal{W}_2$ and the straight line:

$$\left\{t\left(N+1-\text{rank}(X_{1,j}),N+1-\text{rank}(X_{2,j}),N+1-\text{rank}(X_{3,j})\right):t\in\mathbb{R}\right\}.$$

Assigning equal weights to these intersection points yields an empirical estimate of the spectral measure H on $\mathcal{W}_2$.

To examine the reasonableness of the derived limits as approximations of the CTE-based and GTE-based allocations when the confidence level q is close to one, Tables 8–10 report the absolute differences between the allocation limits and the empirical estimates obtained using the method proposed in Gribkova et al. (2022b), under varying assumed values of the common tail index α. We observe that across all dimensions, the differences between the allocation limits based on Theorem 4.2 and those based on the empirical estimator decrease as the confidence level q increases. This suggests that the derived limits appropriately capture the convergence trend of the CTE-based and GTE-based allocations as q approaches one.

Admittedly, the results presented in Tables 8–10 serve primarily to illustrate the trend of convergence. They may not be sufficient to demonstrate that the allocation limits perfectly match the empirical estimates as the confidence level q approaches one. Such precise validation is typically difficult in real data applications due to finite sample sizes, data noise, and imperfect adherence to the tail assumptions underlying the theoretical framework. However, we observe that when $q=0.95$, the differences between the allocation limits and the empirical estimates are already quite small.

Assumed common tail index $\hat{\alpha}$		1.2	1.4	1.6	1.8	1.9
Allocation limit		32.60%	36.93%	36.32%	37.05%	35.02%
Difference with empirical estimate of the CTE-based allocation	$q=0.1$	0.2071	0.1638	0.1698	**0.1626**	0.1829
	$q=0.5$	0.1679	0.1245	0.1306	**0.1234**	0.1436
	$q=0.8$	0.1085	0.0652	0.0712	**0.0640**	0.0843
	$q=0.95$	0.0415	**0.0019**	0.0042	0.0031	0.0172
Difference with empirical estimate of the GTE-based allocation	$q=0.1$	0.3288	0.2854	0.2915	**0.2843**	0.3046
	$q=0.5$	0.2740	0.2306	0.2367	**0.2295**	0.2497
	$q=0.8$	0.1744	0.1311	0.1371	**0.1299**	0.1502
	$q=0.95$	0.0400	0.0034	**0.0027**	0.0045	0.0157

Table 8: Summary of the absolute differences between the allocation limit computed via Theorem 4.2 and the empirical estimates of the CTE-based and GTE-based allocations for the building coverage with claim variable X_1. For each confidence level q, the smallest absolute difference across different values of α is highlighted in bold.

Moreover, among the different values of the common tail index assumed in the MRV framework, we observe that $\hat{\alpha}=1.6$ or $\hat{\alpha}=1.8$ typically yield the smallest absolute differences between the allocation limit and the empirical estimates. We argue that these values represent the "optimal" choice in the sense that they provide the

Assumed common tail index $\hat{\alpha}$		1.2	1.4	1.6	1.8	1.9
Allocation limit		50.49%	49.48%	50.43%	48.86%	51.52%
Difference with empirical estimate of the CTE-based allocation	$q = 0.1$	0.1111	0.1010	0.1106	**0.0948**	0.1214
	$q = 0.5$	0.0810	0.0710	0.0805	**0.0647**	0.0914
	$q = 0.8$	0.0345	0.0244	0.0340	**0.0182**	0.0448
	$q = 0.95$	0.0165	0.0265	0.0170	0.0328	**0.0061**
Difference with empirical estimate of the GTE-based allocation	$q = 0.1$	0.2039	0.1939	0.2034	**0.1876**	0.2143
	$q = 0.5$	0.1619	0.1518	0.1614	**0.1456**	0.1722
	$q = 0.8$	0.0814	0.0713	0.0809	**0.0651**	0.0917
	$q = 0.95$	0.0311	0.0412	0.0317	0.0474	**0.0208**

Table 9: Summary of the absolute differences between the allocation limit computed via Theorem 4.2 and the empirical estimates of the CTE-based and GTE-based allocations for the content coverage with claim variable X_2. For each confidence level q, the smallest absolute difference across different values of α is highlighted in bold.

Assumed common tail index $\hat{\alpha}$		1.2	1.4	1.6	1.8	1.9
Allocation limit		16.92%	13.59%	13.24%	14.10%	13.46%
Difference with empirical estimate of the CTE-based allocation	$q = 0.1$	0.0960	0.0627	**0.0593**	0.0678	0.0615
	$q = 0.5$	0.0868	0.0535	**0.0501**	0.0586	0.0523
	$q = 0.8$	0.0740	0.0407	**0.0373**	0.0458	0.0385
	$q = 0.95$	0.0579	0.0246	**0.0212**	0.0297	0.0234
Difference with empirical estimate of the GTE-based allocation	$q = 0.1$	0.1245	0.0912	**0.0877**	0.0963	0.0899
	$q = 0.5$	0.1116	0.0783	**0.0749**	0.0834	0.0771
	$q = 0.8$	0.0916	0.0583	**0.0549**	0.0634	0.0571
	$q = 0.95$	0.0651	0.0318	**0.0283**	0.0369	0.0305

Table 10: Summary of the absolute differences between the allocation limit computed via Theorem 4.2 and the empirical estimates of the CTE-based and GTE-based allocations for the profit coverage with claim variable X_3. For each confidence level q, the smallest absolute difference across different values of α is highlighted in bold.

best asymptotic approximation, assuming the data distribution indeed follows an MRV structure.

Recall that, due to the asymptotic equivalence between the two allocation methods, in Section 6, we demonstrated through numerical simulations that the GTE-based allocation serves as a robust alternative to the CTE-based allocation, as its estimator exhibits lower variance. However, unlike in simulation settings where an arbitrary number of samples can be generated, real-data applications are constrained to a single observed dataset with a fixed sample size. To compare the robustness of the empirical estimators for the two allocation methods in this real data example, we employ the bootstrap method, which is known to be consistent for estimating the coverage probabilities of tail-based allocations (Gribkova et al., 2024). Specifically, we repeatedly sample with replacement from the original data to generate $L = 500$ bootstrap datasets, each of size N. The empirical estimator from Gribkova et al. (2022b) is then applied to each bootstrap sample to compute both the CTE-based and GTE-based allocation

estimates. These $L = 500$ pairs of estimates yield confidence intervals for the two methods, which are summarized in the box plots in Figure 5.

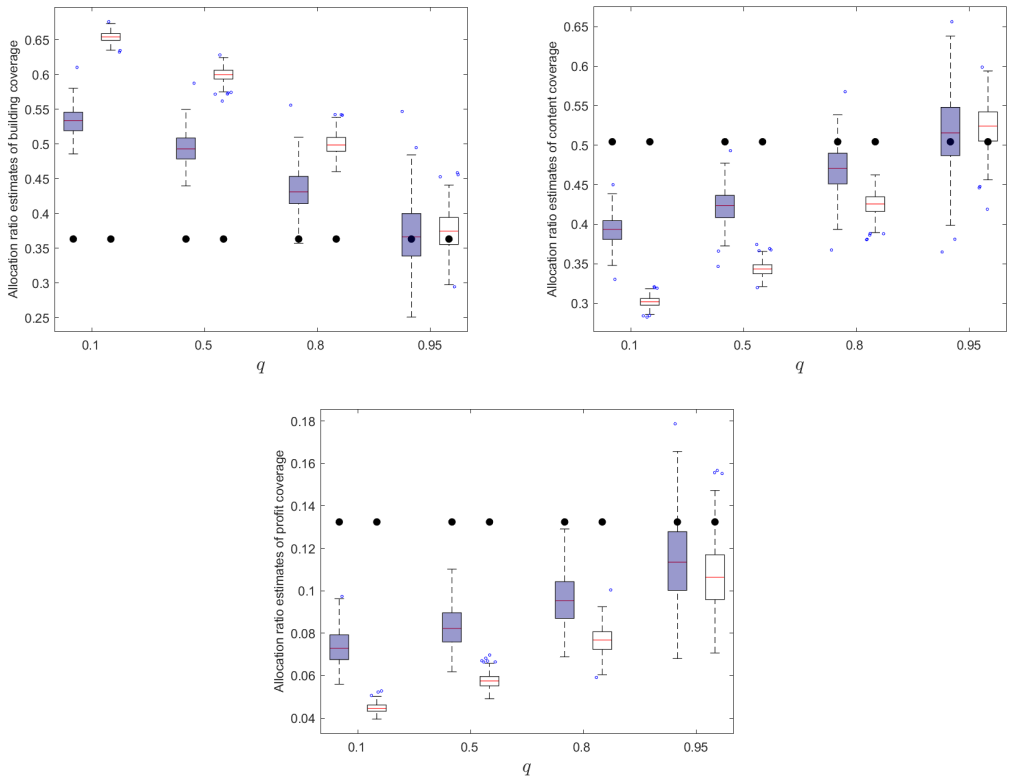

Figure 5: Box plots of the CTE-based allocation estimates (filled boxes) and GTE-based allocation estimates (blank boxes) for X_1 (top-left), X_2 (top-right), and X_3 (bottom-middle), at varying confidence levels. The black dots represent the limits of the two allocation methods computed under $\hat{\alpha} = 1.6$.

We make the following observations. First, when the confidence level q is low, the CTE-based and GTE-based allocation estimates differ noticeably, with entirely disjoint confidence intervals. However, as the confidence level increases, the mean estimates of the two methods align, and their confidence intervals begin to overlap, which is consistent with the asymptotic parity result established in our theoretical analysis. Second, while the variability of the two estimators is comparable at lower confidence levels, at higher confidence levels, the variance of the GTE-based estimator is clearly smaller than that of the CTE-based estimator, underscoring the statistical advantage of the GTE-based allocation method.

8 Conclusions

The GTE risk measure is a newly developed, relative, and robust alternative to the widely advocated CTE risk measure. This paper examines the asymptotic behavior of a proportional allocation scheme induced by the GTE risk

measure. We consider a variety of asymptotic scenarios, encompassing both tail dependence and tail independence, while accommodating marginal distributions that exhibit either heavy or light tails. We derive the limit of the GTE-based allocation and find that, although for fixed $q \in (0,1)$ it differs from the CTE-based allocation, for q close to 1, they are the same asymptotically under all scenarios considered in this paper. In fact, whether they can differ for $q \uparrow 1$ and under what scenarios they may differ remain some highly nontrivial open questions.

We illustrate through extensive numerical simulations and real-data analysis that the variance of the empirical estimator for the GTE-based allocation method is significantly smaller than that of the CTE-based method. Owing to the asymptotic equivalence between the two allocation approaches, our analysis suggests that the GTE-based method can serve as a robust alternative to the CTE-based method when a sufficiently high confidence level is considered. Admittedly, the statistical robustness of the GTE-based method is observed empirically through numerical analysis. Future research should aim to formalize this observation and investigate its theoretical foundation.

Acknowledgment

Owada's research was partially supported by the AFOSR grant FA9550-22-1-0238 at Purdue University.

References

Asimit, A. V. and Badescu, A. L. (2010). Extremes on the discounted aggregate claims in a time dependent risk model. *Scandinavian Actuarial Journal*, 2010(2):93–104.

Asimit, A. V., Furman, E., Tang, Q., and Vernic, R. (2011). Asymptotics for risk capital allocations based on Conditional Tail Expectation. *Insurance: Mathematics and Economics*, 49(3):310–324.

Barbe, P., Fougeres, A.-L., and Genest, C. (2006). On the tail behavior of sums of dependent risks. *ASTIN Bulletin: The Journal of the IAA*, 36(2):361–373.

Bauer, D. and Zanjani, G. (2016). The marginal cost of risk, risk measures, and capital allocation. *Management Science*, 62(5):1431–1457.

Belles-Sampera, J., Guillen, M., and Santolino, M. (2016). Compositional methods applied to capital allocation problems. *Journal of Risk*, 19(2):15–30.

Bellini, F., Laeven, R. J., and Rosazza Gianin, E. (2018). Robust return risk measures. *Mathematics and Financial Economics*, 12(1):5–32.

Boonen, T. J., Guillen, M., and Santolino, M. (2019). Forecasting compositional risk allocations. *Insurance: Mathematics and Economics*, 84:79–86.

Chavez-Demoulin, V., Embrechts, P., and Hofert, M. (2016). An extreme value approach for modeling operational risk losses depending on covariates. *Journal of Risk and Insurance*, 83(3):735–776.

Chen, Y., Embrechts, P., and Wang, R. (2025). An unexpected stochastic dominance: Pareto distributions, dependence, and diversification. *Operations Research*, 73(3):1336–1344.

Chen, Y. and Liu, J. (2022). An asymptotic study of systemic expected shortfall and marginal expected shortfall. *Insurance: Mathematics and Economics*, 105:238–251.

Chen, Y. and Liu, J. (2024). Asymptotic capital allocation based on the higher moment risk measure. *European Actuarial Journal*, 14:657–684.

Chen, Y. and Wang, R. (2025). Infinite-mean models in risk management: Discussions and recent advances. *Risk Sciences*, 1:100003.

Cui, H., Tan, K. S., and Yang, F. (2024). Portfolio credit risk with Archimedean copulas: Asymptotic analysis and efficient simulation. *Annals of Operations Research*, 332(1):55–84.

Das, B., Mitra, A., and Resnick, S. (2013). Living on the multidimensional edge: Seeking hidden risks using regular variation. *Advances in Applied Probability*, 45(1):139–163.

Das, B. and Resnick, S. I. (2017). Hidden regular variation under full and strong asymptotic dependence. *Extremes*, 20(4):873–904.

Denault, M. (2001). Coherent allocation of risk capital. *Journal of Risk*, 4(1):1–34.

Dhaene, J., Tsanakas, A., Valdez, E. A., and Vanduffel, S. (2012). Optimal capital allocation principles. *Journal of Risk and Insurance*, 79(1):1–28.

Einmahl, J. H., Yang, F., and Zhou, C. (2021). Testing the multivariate regular variation model. *Journal of Business & Economic Statistics*, 39(4):907–919.

Embrechts, P., Klüppelberg, C., and Mikosch, T. (1997). *Modelling Extremal Events*. Springer, Heidelberg.

Fiori, A. M. and Rosazza Gianin, E. (2025). Compositional risk capital allocations. *Statistical Methods and Applications*, 34(2):261–290.

Furman, E., Kye, Y., and Su, J. (2021). A reconciliation of the top-down and bottom-up approaches to risk capital allocations: Proportional allocations revisited. *North American Actuarial Journal*, 25(3):395–416.

Furman, E. and Zitikis, R. (2008). Weighted risk capital allocations. *Insurance: Mathematics and Economics*, 43(2):263–269.

Gribkova, N., Su, J., and Zitikis, R. (2022a). Empirical tail conditional allocation and its consistency under minimal assumptions. *Annals of the Institute of Statistical Mathematics*, 74:713–735.

Gribkova, N., Su, J., and Zitikis, R. (2022b). Inference for the tail conditional allocation: Large sample properties, insurance risk assessment, and compound sums of concomitants. *Insurance: Mathematics and Economics*, 107:199–222.

Gribkova, N., Su, J., and Zitikis, R. (2024). Assessing the coverage probabilities of fixed-margin confidence intervals for the tail conditional allocation. *Annals of the Institute of Statistical Mathematics*, 76(5):821–850.

Guo, Q., Bauer, D., and Zanjani, G. (2021). Capital allocation techniques: Review and comparison. *Variance*, 14(2):1–32.

Hua, L. and Joe, H. (2011a). Second order regular variation and conditional tail expectation of multiple risks. *Insurance: Mathematics and Economics*, 49(3):537–546.

Hua, L. and Joe, H. (2011b). Tail order and intermediate tail dependence of multivariate copulas. *Journal of Multivariate Analysis*, 102(10):1454–1471.

Hua, L. and Joe, H. (2012). Tail comonotonicity: Properties, constructions, and asymptotic additivity of risk measures. *Insurance: Mathematics and Economics*, 51(2):492–503.

Kalkbrener, M. (2005). An axiomatic approach to capital allocation. *Mathematical Finance*, 15(3):425–437.

Laeven, R. J., Gianin, E. R., and Zullino, M. (2024). Law-invariant return and star-shaped risk measures. *Insurance: Mathematics and Economics*, 117:140–153.

Laeven, R. J. and Goovaerts, M. J. (2004). An optimization approach to the dynamic allocation of economic capital. *Insurance: Mathematics and Economics*, 35(2):299–319.

Laeven, R. J. and Rosazza Gianin, E. (2022). Quasi-logconvex measures of risk. *arXiv preprint: 2208.07694*.

Lehtomaa, J. and Resnick, S. I. (2020). Asymptotic independence and support detection techniques for heavy-tailed multivariate data. *Insurance: Mathematics and Economics*, 93:262–277.

Li, J., Tang, Q., and Wu, R. (2010). Subexponential tails of discounted aggregate claims in a time-dependent renewal risk model. *Advances in Applied Probability*, 42(4):1126–1146.

Lindskog, F., Resnick, S. I., and Roy, J. (2014). Regularly varying measures on metric spaces: Hidden regular variation and hidden jumps. *Probability Surveys*, 11(2014):270–314.

Malavasi, M., Peters, G. W., Shevchenko, P. V., Trück, S., Jang, J., and Sofronov, G. (2022). Cyber risk frequency, severity and insurance viability. *Insurance: Mathematics and Economics*, 106:90–114.

Mao, T., Stupfler, G., and Yang, F. (2023). Asymptotic properties of generalized shortfall risk measures for heavy-tailed risks. *Insurance: Mathematics and Economics*, 111:173–192.

McNeil, A. J. (1997). Estimating the tails of loss severity distributions using extreme value theory. *ASTIN Bulletin: The Journal of the IAA*, 27(1):117–137.

McNeil, A. J., Frey, R., and Embrechts, P. (2015). *Quantitative Risk Management: Concepts, Techniques and Tools*. Princeton University Press: Princeton.

Mitra, A. and Resnick, S. I. (2009). Aggregation of rapidly varying risks and asymptotic independence. *Advances in Applied Probability*, 41(3):797–828.

Mohammed, N., Furman, E., and Su, J. (2021). Can a regulatory risk measure induce profit-maximizing risk capital allocations? The case of conditional tail expectation. *Insurance: Mathematics and Economics*, 101:425–436.

Moscadelli, M. (2004). The modelling of operational risk: experience with the analysis of the data collected by the basel committee. *Available at SSRN 557214*.

NAIC (2012). Risk-based capital (RBC) for insurers model act. National Association of Insurance Commissioners, Technical Report.

OSFI (2017). Own risk and solvency assessment (ORSA) guideline. Office of the Superintendent of Financial Institutions, Technical Report.

Qin, X. and Zhou, C. (2021). Systemic risk allocation using the asymptotic marginal expected shortfall. *Journal of Banking and Finance*, 126:106099.

Resnick, S. I. (1997). Discussion of the danish data on large fire insurance losses. *ASTIN Bulletin: The Journal of the IAA*, 27(1):139–151.

Resnick, S. I. (2007). *Heavy-Tail Phenomena: Probabilistic and Statistical Modeling*. Springer: New York.

Resnick, S. I. (2008). *Extreme Values, Regular Variation, and Point Processes*. Springer: New York.

Tang, Q. and Yuan, Z. (2013). Asymptotic analysis of the loss given default in the presence of multivariate regular variation. *North American Actuarial Journal*, 17(3):253–271.

Tsanakas, A. and Barnett, C. (2003). Risk capital allocation and cooperative pricing of insurance liabilities. *Insurance: Mathematics and Economics*, 33:239–254.

Zhu, L. and Li, H. (2012a). Asymptotic analysis of multivariate tail conditional expectations. *North American Actuarial Journal*, 16(3):350–363.

Zhu, L. and Li, H. (2012b). Tail distortion risk and its asymptotic analysis. *Insurance: Mathematics and Economics*, 51(1):115–121.

Appendix A Technical proofs

Proof of Theorem 4.2. By equation (5), we have, for every $i \in \mathcal{N}$,

$$\lim_{q\uparrow 1} \tilde{r}_{i,q} = \lim_{q\uparrow 1} E(R_i \,|\, S > s_q) = \lim_{t\to\infty} E(R_i \,|\, S > t), \tag{28}$$

where $t = s_q$. Since R_i given by (6) is nonnegative, we have

$$E(R_i \,|\, S > t) = \int_0^1 P(R_i > z \,|\, S > t)\, \mathrm{d}z = \int_0^1 \frac{P(X_i > Sz, S > t)\,/\,\overline{F}_1(t)}{P(S > t)\,/\,\overline{F}_1(t)}\, \mathrm{d}z. \tag{29}$$

On the one hand, it is well known (Resnick, 2007, Proposition 7.3) that under condition ($\mathbf{C}_1$), $P(S > t) \sim \mu(\aleph)\overline{F}_1(t)$, where $0 < \mu(\aleph) < \infty$ because $\mu \in \mathbb{M}\left(\mathbb{R}_+^n \setminus \{\mathbf{0}\}\right)$.

On the other hand, to examine the numerator in the last term of (29), write $B_z = \{\boldsymbol{x} \in [\mathbf{0}, \boldsymbol{\infty}) : x_i = z \sum_{k=1}^n x_k, \sum_{k=1}^n x_k > 1\}$ for $z \in [0,1]$ and $\mathcal{Z} = \{z \in (0,1] : \mu(B_z) > 0\}$; that is, $\mathcal{Z}$ is the collection of points z in $(0,1]$ such that the measure μ assigns a positive mass to the set B_z. We claim that there are at most countably many elements in $\mathcal{Z}$. To see this, for $n = 1, 2, \ldots$, write $\mathcal{Z}_n = \{z \in \mathcal{Z} : \mu(B_z) \geq 1/n\}$. If there are uncountably many elements in $\mathcal{Z}$, then, since the union of countably many sets with finite members is at most countable, there exists a positive integer n_0, such that $\mathcal{Z}_{n_0}$ has infinite members, and hence has a countable subset $\mathcal{Z}_{n_0}^c$ with infinite members. Since $B_{z_1} \bigcap B_{z_2} = \emptyset$ for any $z_1 \neq z_2$, this implies $\mu\big(\bigcup_{z\in\mathcal{Z}_{n_0}^c} B_z\big) = \sum_{z\in\mathcal{Z}_{n_0}^c} \mu(B_z) = \infty$. However, noticing that $\bigcup_{z\in[0,1]} B_z = \aleph$ and that B_z's are disjoint, we have $\mu\big(\bigcup_{z\in\mathcal{Z}_{n_0}^c} B_z\big) \leq \mu\big(\bigcup_{z\in[0,1]} B_z\big) = \mu(\aleph) < \infty$, which is a contradiction. Hence, the set $\mathcal{Z}$ has at most countably many members.

For every $z \in (0,1] \setminus \mathcal{Z}$, we have

$$\begin{aligned}\mu(\partial A_{i,z}) &= \mu\left(B_z \bigcup \left\{\boldsymbol{x} \in [\mathbf{0},\boldsymbol{\infty}) : x_i > z\sum_{k=1}^{n} x_k, \sum_{k=1}^{n} x_k = 1\right\}\right) \\ &\leq \mu(B_z) + \mu\left(\left\{\boldsymbol{x} \in [\mathbf{0},\boldsymbol{\infty}) : \sum_{k=1}^{n} x_k = 1\right\}\right) \\ &= 0. \end{aligned} \tag{30}$$

Hence, it holds for $z \in (0,1] \setminus \mathcal{Z}$ that

$$\begin{aligned}\lim_{t\to\infty} \frac{P(X_i > Sz, S > t)}{\overline{F}_1(t)} &= \lim_{t\to\infty} \frac{P(X_i/t > Sz/t, S/t > 1)}{\overline{F}_1(t)} \\ &= \mu\left(\boldsymbol{x} \in [\mathbf{0},\boldsymbol{\infty}) : x_i > z\sum_{k=1}^{n} x_k, \sum_{k=1}^{n} x_k > 1\right) \\ &= \mu(A_{i,z}),\end{aligned}$$

where in the last step, we used equations (11) and (30). Thus,

$$\begin{aligned}\lim_{t\to\infty} E(R_i \,|\, S > t) &= \lim_{t\to\infty} \int_{(0,1]\setminus\mathcal{Z}} \frac{P(X_i > Sz, S > t)/\overline{F}_1(t)}{P(S > t)/\overline{F}_1(t)} \,\mathrm{d}z \\ &= \int_{(0,1]\setminus\mathcal{Z}} \lim_{t\to\infty} \frac{P(X_i > Sz, S > t)/\overline{F}_1(t)}{P(S > t)/\overline{F}_1(t)} \,\mathrm{d}z \\ &= \int_{(0,1]\setminus\mathcal{Z}} \frac{\mu(A_{i,z})}{\mu(\aleph)} \,\mathrm{d}z \\ &= \int_0^1 \frac{\mu(A_{i,z})}{\mu(\aleph)} \,\mathrm{d}z,\end{aligned}$$

where in the first and last steps we used the fact that $\mathcal{Z}$ has at most countable members, and in the second step we used the Dominated Convergence Theorem. This completes the proof. □

Proof of Proposition 4.3. We use the idea of Barbe et al. (2006) to prove the proposition. Write $b_i(\cdot) = \left(1/\overline{F}_i\right)^{\leftarrow}(\cdot)$ and note that, for any $z \in (0,1]$,

$$P(X_i > zS, S > t) = P\left(b_i(Y_i) > z\sum_{k=1}^{n} b_k(Y_k), \sum_{k=1}^{n} b_k(Y_k) > t\right) = P\left(\frac{Y}{s} \in A^*_{z,t}\right),$$

where $s = 1/\overline{F}_1(t)$ and $A^*_{z,t} = \left\{a \in \mathbb{R}^n_+ : b_i(a_i s) > z\sum_{k=1}^{n} b_k(a_k s), \sum_{k=1}^{n} b_k(a_k s) > t\right\}$. Here we used the facts that $b_i(Y_i) = \left(1/\overline{F}_i\right)^{\leftarrow}\left(1/\overline{F}_i(X_i)\right) = F_i^{\leftarrow}(F_i(X_i))$ and $P(F_i^{\leftarrow}(F_i(X_i)) = X_i) = 1$ (see McNeil et al., 2015, Proposition

A.4) and that copulas are invariant under componentwise-monotone increasing transforms. Recall equation (14), which implies that $b_k(s) \sim c_k^{1/\alpha} b_1(s) \sim c_k^{1/\alpha} t$, $k \in N$. It follows that, for any $i \in N$ and $z \in (0,1]$,

$$\frac{P(X_i > zS, S > t)}{\overline{F}_1(t)} = sP\left(\frac{Y}{s} \in A^*_{z,t}\right) \sim sP\left(\frac{Y}{s} \in A^*_z\right) \to \mu^*\left(A^*_z\right),$$

where $A^*_z = \left\{a \in \mathbb{R}^n_+ : c_i^{1/\alpha} a_i^{1/\alpha} > z\sum_{k=1}^n c_k^{1/\alpha} a_k^{1/\alpha}, \sum_{k=1}^n c_k^{1/\alpha} a_k^{1/\alpha} > 1\right\}$. The proof of Theorem 4.2 shows that the left-hand size tends to $\mu(A_z)$, and hence, $\mu(A_z) = \mu^*\left(A^*_z\right)$. Note that

$$\begin{aligned} T^{-1}\left(A^*_z\right) &= \left\{(r, \boldsymbol{w}) \in (0,\infty) \times \mathcal{W}_{n-1} : c_i^{1/\alpha}(rw_i)^{1/\alpha} > z\sum_{k=1}^n c_k^{1/\alpha}(rw_k)^{1/\alpha}, \sum_{k=1}^n c_k^{1/\alpha}(rw_k)^{1/\alpha} > 1\right\} \\ &= \left\{(r, \boldsymbol{w}) \in (0,\infty) \times \mathcal{W}_{n-1} : c_i^{1/\alpha} w_i^{1/\alpha} > z\sum_{k=1}^n c_k^{1/\alpha} w_k^{1/\alpha}, r > \left(\sum_{k=1}^n c_k^{1/\alpha} w_k^{1/\alpha}\right)^{-\alpha}\right\}. \end{aligned}$$

Therefore,

$$\begin{aligned} \int_0^1 \mu(A_z)\,\mathrm{d}z &= \int_0^1 \mu^*\left(A^*_z\right)\mathrm{d}z \\ &= n\int_0^1 \int_{\mathcal{W}_{n-1}} 1_{\left(c_i^{1/\alpha} w_i^{1/\alpha} > z\sum_{k=1}^n c_k^{1/\alpha} w_k^{1/\alpha}\right)} \int_{\left(\sum_{k=1}^n c_k^{1/\alpha} w_k^{1/\alpha}\right)^{-\alpha}}^{\infty} r^{-2}\mathrm{d}r H(\mathrm{d}w)\mathrm{d}z \\ &= n\int_0^1 \int_{\mathcal{W}_{n-1}} 1_{\left(c_i^{1/\alpha} w_i^{1/\alpha} > z\sum_{k=1}^n c_k^{1/\alpha} w_k^{1/\alpha}\right)} \left(\sum_{k=1}^n c_k^{1/\alpha} w_k^{1/\alpha}\right)^{\alpha} H(\mathrm{d}w)\mathrm{d}z \\ &= n\int_{\mathcal{W}_{n-1}} \left(\sum_{k=1}^n c_k^{1/\alpha} w_k^{1/\alpha}\right)^{\alpha} \int_0^1 1_{\left(c_i^{1/\alpha} w_i^{1/\alpha} > z\sum_{k=1}^n c_k^{1/\alpha} w_k^{1/\alpha}\right)} \mathrm{d}z H(\mathrm{d}w) \\ &= n\int_{\mathcal{W}_{n-1}} \left(\sum_{k=1}^n c_k^{1/\alpha} w_k^{1/\alpha}\right)^{\alpha} \frac{c_i^{1/\alpha} w_i^{1/\alpha}}{\sum_{k=1}^n c_k^{1/\alpha} w_k^{1/\alpha}} H(\mathrm{d}w) \\ &= n\int_{\mathcal{W}_{n-1}} c_i^{1/\alpha} w_i^{1/\alpha} \left(\sum_{k=1}^n c_k^{1/\alpha} w_k^{1/\alpha}\right)^{\alpha-1} H(\mathrm{d}w). \end{aligned}$$

Similarly, we can show that

$$\mu(\aleph) = n\int_{\mathcal{W}_{n-1}} \left(\sum_{k=1}^n c_k^{1/\alpha} w_k^{1/\alpha}\right)^{\alpha} H(\mathrm{d}w).$$

Together, this leads to an allocation to the ith line of

$$\frac{\int_{\mathcal{W}_{n-1}} c_i^{1/\alpha} w_i^{1/\alpha} \left(\sum_{k=1}^n c_k^{1/\alpha} w_k^{1/\alpha}\right)^{\alpha-1} H(\mathrm{d}w)}{\int_{\mathcal{W}_{n-1}} \left(\sum_{k=1}^n c_k^{1/\alpha} w_k^{1/\alpha}\right)^{\alpha} H(\mathrm{d}w)},$$

which completes the proof. □

Proof of Proposition 4.5. The proof is similar to that of Theorem 8.3 of Das et al. (2013) but is adapted for the case with Gumbel marginals.

Write $\mathbb{D} = [-\infty,\infty)^n \setminus \{-\boldsymbol{\infty}\}$ and $\mathbb{E} = [-\infty,\infty]^n \setminus \{-\boldsymbol{\infty}\}$. On the one hand, suppose that the vague convergence in relation (18) holds with auxiliary function $a(\cdot)$ and limit measure ν. We know that the limit measure ν assigns no mass to the lines through $\boldsymbol{\infty}$. To see this, note that, for every $x_i > -\infty$,

$$\mu([-\infty,\infty] \times \cdots \times (x_i,\infty] \times \cdots \times [-\infty,\infty]) = \lim_{t\to\infty} \frac{P((X_i - t)/a(t) > x_i)}{\overline{F}_1(t)} = c_i e^{-x_i}, \tag{31}$$

where $c_i = \mu(\boldsymbol{x} : x_i > 0)$, and hence, the total mass assigned to the lines through $\boldsymbol{\infty}$ is not greater than

$$\lim_{x\to\infty} \sum_{i=1}^{n} \mu([-\infty,\infty] \times \cdots \times (x,\infty] \times \cdots \times [-\infty,\infty]) = \lim_{x\to\infty} \sum_{i=1}^{n} c_i e^{-x} = 0.$$

Now define a measure χ_m on $\mathbb{D}$ by $\chi_m(\cdot) = \nu(\cdot)$. Since ν is nonzero and nondegenerate and assigns zero mass to $\mathbb{E} \setminus \mathbb{D}$, we know χ_m is also nonzero and nondegenerate. Moreover, for $A \subset \mathbb{D}$ bounded away from $\{-\boldsymbol{\infty}\}$ with $\chi_m(\partial A) = 0$, it follows from Proposition 6.1 of Resnick (2007) that A is relatively compact in $\mathbb{E}$ with $\nu(\partial A) = 0$. Therefore, relation (18) implies that

$$P((\boldsymbol{X} - t\mathbf{1})/a(t) \in A)/\overline{F}_1(t) \to \nu(A) = \chi_m(A),$$

and hence, by Theorem 2.1 of Lindskog et al. (2014), the $\mathbb{M}$ convergence in (17) holds with limit measure $\mu = \chi_m$ and the same auxiliary function $a(\cdot)$.

On the other hand, suppose that the $\mathbb{M}$ convergence in (17) holds with auxiliary function $a(\cdot)$ and limit measure μ. Define a measure χ_v on $\mathbb{E}$ such that $\chi_v(\cdot) = \mu(\cdot \cap \mathbb{D})$. Since μ is nonzero and nondegenerate, so is χ_v. Now consider an arbitrary set $A \subset \mathbb{E}$ with $\chi_v(\partial A) = 0$ that is relatively compact in $\mathbb{E}$. By Proposition 6.1 of Resnick (2007), A is bounded away from $\{-\boldsymbol{\infty}\}$. Moreover, we have $\mu(\partial(A \cap \mathbb{D})) = \mu(\partial A \cap \mathbb{D}) = \chi_v(\partial A) = 0$. Hence, relation (18) implies that

$$\frac{P((\boldsymbol{X} - t\mathbf{1})/a(t) \in A)}{\overline{F}_1(t)} = \frac{P((\boldsymbol{X} - t\mathbf{1})/a(t) \in A \cap \mathbb{D})}{\overline{F}_1(t)} \to \nu(A \cap \mathbb{D}) = \chi_v(A).$$

This means that the vague convergence given by (18) holds with limit measure $\nu = \chi_v$ and the same auxiliary function $a(\cdot)$.

The proof is now completed. □

Proof of Theorem 4.6. By equation (5), we have, for every $i \in \mathcal{N}$,

$$\lim_{q\uparrow 1} \tilde{r}_{i,q} = \lim_{q\uparrow 1} E(R_i \,|\, S > s_q) = \lim_{t\to\infty} E(R_i \,|\, S > nt),$$

where $t = s_q/n$. First note that $R_i \geq 0$ and consider

$$\begin{aligned}
E(R_i \,|\, S > nt) &= \int_0^1 P(R_i > z \,|\, S > nt)\,\mathrm{d}z \\
&= \int_0^1 \frac{P(X_i > Sz, S > nt)}{P(S > nt)}\,\mathrm{d}z \\
&= \int_0^{1/n} \frac{1}{P(S > nt)} P\left(\frac{X_i - t}{a(t)} > z\frac{S-nt}{a(t)} + \frac{(nz-1)t}{a(t)}, \frac{S-nt}{a(t)} > 0\right)\mathrm{d}z \\
&\quad + \int_{1/n}^1 \frac{1}{P(S > nt)} P\left(\frac{X_i - t}{a(t)} > z\frac{S-nt}{a(t)} + \frac{(nz-1)t}{a(t)}, \frac{S-nt}{a(t)} > 0\right)\mathrm{d}z \\
&=: I_1(t) + I_2(t).
\end{aligned}$$

Given any $\varepsilon > 0$ fixed, we have $a(t) < \varepsilon t$ for t sufficiently large. It follows that

$$\begin{aligned}
\limsup_{t\to\infty} I_2(t) &= \limsup_{t\to\infty} \int_{1/n}^1 \frac{1}{P(S > nt)} P\left(\frac{X_i - t}{a(t)} > z\frac{S-nt}{a(t)} + \frac{(nz-1)t}{a(t)}, \frac{S-nt}{a(t)} > 0\right)\mathrm{d}z \\
&\leq \int_{1/n}^1 \limsup_{t\to\infty} \frac{1}{P(S > nt)} P\Big(\frac{X_i - t}{a(t)} > z\frac{S-nt}{a(t)} + \frac{nz-1}{\varepsilon}, \frac{S-nt}{a(t)} > 0\Big)\mathrm{d}z \\
&\leq \int_{1/n}^1 \limsup_{t\to\infty} \frac{P\Big((X_i - t)/a(t) > (nz-1)/\varepsilon\Big)/\overline{F}_1(t)}{P(S > nt)/\overline{F}_1(t)}\,\mathrm{d}z \\
&= \int_{1/n}^1 \frac{\mu\Big(\boldsymbol{x} : x_i > (nz-1)/\varepsilon\Big)}{\mu\Big(\boldsymbol{x} : \sum_{k=1}^n x_k > 0\Big)}\mathrm{d}z \\
&= \frac{\int_{1/n}^1 c_i e^{-(nz-1)/\varepsilon}\mathrm{d}z}{\mu\Big(\boldsymbol{x} : \sum_{k=1}^n x_k > 0\Big)} \\
&\leq \frac{c_i\,\varepsilon}{n\mu\Big(\boldsymbol{x} : \sum_{k=1}^n x_k > 0\Big)},
\end{aligned}$$

where the second step follows from Fatou's lemma and the fact that the integrand on the left-hand size is not greater than 1, the fourth step is due to condition ($\mathbf{C}_2$) and equation (20), and the fifth step arises from equation (31). By the arbitrariness of ε, we have $I_2(t) \to 0$.

Now let us consider $I_1(t)$. It is obvious that $I_1(t) \leq 1/n$ and we now show that $\liminf_{t\to\infty} I_1(t) \geq 1/n$. Note that,

for every $z \in (0,1]$,

$$P\left(\frac{X_i - t}{a(t)} > z\frac{S-nt}{a(t)} + \frac{nz-1}{\varepsilon}, \frac{S-nt}{a(t)} > 0\right) = P\left(\frac{\boldsymbol{X} - t\mathbf{1}}{a(t)} \in A_z\right),$$

where $A_z = \{\boldsymbol{x} \in (-\infty,\infty) : x_i > z\sum_{k=1}^n x_k + (nz-1)/\varepsilon, \sum_{k=1}^n x_k > 0\}$. Write $\mathcal{Z} = \{z \in (0,1] : \mu(\partial A_z) > 0\}$ and $\mathcal{Z}^c = (0,1] \setminus \mathcal{Z}$. Using a similar argument to that in the proof of Theorem 4.2, we can verify that there are at most countably many elements in $\mathcal{Z}$. Therefore,

$$\begin{aligned}
\liminf_{t\to\infty} I_1(t) &= \liminf_{t\to\infty} \int_{(0,1/n]\cap\mathcal{Z}^c} \frac{1}{P(S>nt)} P\left(\frac{X_i - t}{a(t)} > z\frac{S-nt}{a(t)} + \frac{(nz-1)t}{a(t)}, \frac{S-nt}{a(t)} > 0\right) \mathrm{d}z \\
&\geq \int_{(0,1/n]\cap\mathcal{Z}^c} \liminf_{t\to\infty} \frac{1}{P(S>nt)} P\left(\frac{X_i - t}{a(t)} > z\frac{S-nt}{a(t)} + \frac{(nz-1)t}{a(t)}, \frac{S-nt}{a(t)} > 0\right) \mathrm{d}z \\
&\geq \int_{(0,1/n]\cap\mathcal{Z}^c} \liminf_{t\to\infty} \frac{P\left((\boldsymbol{X} - t\mathbf{1})/a(t) \in A_z\right)/\overline{F}_1(t)}{P(S>nt)/\overline{F}_1(t)} \mathrm{d}z \\
&= \int_{(0,1/n]\cap\mathcal{Z}^c} \frac{\mu(A_z)}{\mu(\boldsymbol{x} : \sum_{k=1}^n x_k > 0)} \mathrm{d}z \\
&= \int_0^{1/n} \frac{\mu(A_z)}{\mu(\boldsymbol{x} : \sum_{k=1}^n x_k > 0)} \mathrm{d}z \\
&\geq \frac{1}{n} - \frac{\int_0^{1/n} \mu\left(\boldsymbol{x} : x_i \leq \sum_{k=1}^n x_k + \frac{nz-1}{\varepsilon}\right) \mathrm{d}z}{\mu\left(\boldsymbol{x} : \sum_{k=1}^n x_k > 0\right)},
\end{aligned} \tag{32}$$

where in the first and fifth steps, we used the fact that $\mathcal{Z}$ has countably many elements, in the second step we used Fatou's lemma, and in the fourth step we used the $\mathbb{M}$ convergence in condition ($\mathbf{C}_2$), equation (20), and the fact that $\mu(\partial A_z) = 0$ for $z \in \mathcal{Z}^c$. Further note that, by equation (31),

$$\mu\left(\boldsymbol{x} : x_i \leq \sum_{k=1}^n x_k + \frac{nz-1}{\varepsilon}\right) = \mu\left(\boldsymbol{x} : \sum_{k=1,k\neq i}^n x_k \geq -\frac{nz-1}{\varepsilon}\right) \leq \sum_{k=1,k\neq i}^n \mu\left(\boldsymbol{x} : x_k \geq -\frac{nz-1}{(n-1)\varepsilon}\right) \to 0$$

as $\varepsilon \to 0$. It follows from (32) that $\liminf_{t\to\infty} I_1(t) \geq 1/n$, and hence, we can conclude $\lim_{t\to\infty} I_1(t) = 1/n$.

This completes the proof. □

Proof of Theorem 5.2. Following the proof of Theorem 4.2, we see that

$$\lim_{q\uparrow 1} \tilde{r}_{i,q} = \lim_{t\to\infty} E(R_i \,|\, S > t) = \int_0^1 \frac{\mu_I(A_{i,z})}{\mu_I(\aleph)} \mathrm{d}z,$$

where $A_{i,z} = \left\{\boldsymbol{x} \in \mathbb{R}_+^n : x_i > z\sum_{k=1}^n x_k, \sum_{k=1}^n x_k > 1\right\}$ and $\aleph = \left\{\boldsymbol{x} \in \mathbb{R}_+^n : \sum_{k=1}^n x_k > 1\right\}$. Since μ_I puts mass on the

axes only, we have

$$\mu_I(\aleph) = \sum_{k=1}^{n} \mu_I\left(\boldsymbol{x} \in \mathbb{R}_+^n : x_k > 1\right) = \sum_{k=1}^{n} c_k, \tag{33}$$

and for $0 < z < 1$,

$$\mu_I(A_{i,z}) = \mu_I(\boldsymbol{x} \in \mathbb{R}_+^n : x_i > 1) = c_i. \tag{34}$$

Combining (33) and (34) yields (21), which completes the proof. □

Proof of Theorem 5.4. First note that equations (28) and (29) remain valid. For $z \in (0,1)$,

$$\begin{aligned}
P(X_i > Sz, S > t) &= P(X_i > Sz, S > t, X_i > zt) \\
&= P(S > t, X_i > zt) - P(Sz \geq X_i, X_i > zt) \\
&= P(S > t, X_i > t) + P(S > t, zt < X_i \leq t) - P(Sz \geq X_i, X_i > t) - P(Sz \geq X_i, zt < X_i \leq t) \\
&= P(X_i > t) + P(S > t, zt < X_i \leq t) - P(Sz \geq X_i, X_i > t) - P(Sz \geq X_i, zt < X_i \leq t).
\end{aligned}$$

Accordingly, we can write

$$\begin{aligned}
&\int_0^1 P(X_i > Sz, S > t)\mathrm{d}z \\
&= P(X_i > t) + \int_0^1 P(S > t, zt < X_i \leq t)\,\mathrm{d}z - \int_0^1 P(Sz \geq X_i, X_i > t)\,\mathrm{d}z - \int_0^1 P(Sz \geq X_i, zt < X_i \leq t)\,\mathrm{d}z \\
&=: I_1(t) + I_2(t) - I_3(t) - I_4(t).
\end{aligned}$$

Obviously, $I_4(t) \leq I_2(t)$, and hence, by (23), it suffices to show

$$I_2(t) = o(1)\,P(S > t) \qquad \text{and} \qquad I_3(t) = o(1)\,P(S > t).$$

We deal with $I_2(t)$ first. Since equation (22) holds uniformly over $x \in [0,\infty)$, for any $\varepsilon > 0$ fixed henceforth, there exists $t_0 > 0$, such that, for all $x > 0$ and $t > t_0$,

$$(1-\varepsilon)\,h_i(x) \sum_{k=1,k\neq i}^{n} \overline{F}_k(t) \;\leq\; P\left(S - X_i > t \,|X_i = x\right) \;\leq\; (1+\varepsilon)\,h_i(x) \sum_{k=1,k\neq i}^{n} \overline{F}_k(t). \tag{35}$$

Therefore, we have

$$\begin{aligned}
I_2(t) &= \int_0^1 \int_{zt}^t P\left(S > t \,|X_i = x\right) F_i(\mathrm{d}x)\,\mathrm{d}z \\
&= \int_0^t \frac{x}{t} P\left(S > t \,|X_i = x\right) F_i(\mathrm{d}x) \\
&= \int_0^{t-t_0} \frac{x}{t} P\left(S > t \,|X_i = x\right) F_i(\mathrm{d}x) + \int_{t-t_0}^t \frac{x}{t} P\left(S > t \,|X_i = x\right) F_i(\mathrm{d}x) \\
&=: I_{21}(t) + I_{22}(t),
\end{aligned}$$

where the second step follows from Fubini's Theorem. Moreover,

$$\begin{aligned}
I_{21}(t) &= \int_0^{t-t_0} \frac{x}{t} P(S - X_i > t - x \,|X_i = x) F_i(\mathrm{d}x) \\
&\le (1+\varepsilon) \sum_{k=1,k\neq i}^n \int_0^{t-t_0} \frac{x}{t} h_i(x) \overline{F}_k(t-x) F_i(\mathrm{d}x) \\
&= (1+\varepsilon) \sum_{k=1,k\neq i}^n \int_0^{1-t_0/t} \int_{zt}^{t-t_0} h_i(x) \overline{F}_k(t-x) F_i(\mathrm{d}x)\mathrm{d}z \\
&= (1+\varepsilon) \sum_{k=1,k\neq i}^n \int_0^{1-t_0/t} \int_{zt}^{t-t_0} \overline{F}_k(t-x) F_i^*(\mathrm{d}x)\mathrm{d}z, \qquad (36)
\end{aligned}$$

where in the third step we used Fubini's Theorem, and the distribution function F_i^* introduced in the last step satisfies $F_i^*(\mathrm{d}x) = h_i(x)F_i(\mathrm{d}x)$. Note that F_i^* is a proper distribution function because $E\left(h_i(X_i)\right) = 1$. Since $\overline{F}_i$ and h_i are regularly varying, F_i^* has a regularly varying tail with an index of, say, $-\alpha_i^* < 0$. Moreover, since h_i is bounded, we have

$$\overline{F}_i^*(t) = O\left(\overline{F}_i(t)\right). \qquad (37)$$

Let us introduce a nonnegative RV $X_i^* \sim F_i^*$ that is independent of $\boldsymbol{X}$. It holds for every $z \in (0,1]$ that

$$\begin{aligned}
\int_{zt}^t \overline{F}_k(t-x) F_i^*(\mathrm{d}x) &= P\left(X_i^* + X_k > t, zt < X_i^* \le t\right) \\
&= P\left(X_i^* + X_k > t\right) - P\left(X_i^* > t\right) - P\left(X_i^* + X_k > t, X_i^* \le zt\right) \\
&\le (1+o(1))(\overline{F}_i^*(t) + \overline{F}_k(t)) - \overline{F}_i^*(t) - \overline{F}_k(t) F_i^*(zt) \\
&= o(1)(\overline{F}_i^*(t) + \overline{F}_k(t)),
\end{aligned}$$

where the second last step follows from Lemma 1.3.1 of Embrechts et al. (1997). Therefore,

$$\begin{aligned}\lim_{t\to\infty}\frac{I_{21}(t)}{P(S>t)} &\le (1+\varepsilon)\sum_{k=1,k\neq i}^{n}\lim_{t\to\infty}\int_0^1\frac{\int_{zt}^{t}\overline{F}_k(t-x)F_i^*(\mathrm{d}x)}{P(S>t)}\mathrm{d}z\\ &\le (1+\varepsilon)\sum_{k=1,k\neq i}^{n}\int_0^1\lim_{t\to\infty}\frac{\int_{zt}^{t}\overline{F}_k(t-x)F_i^*(\mathrm{d}x)}{P(S>t)}\mathrm{d}z\\ &= 0, \end{aligned} \tag{38}$$

where the first step is due to equation (36) and the second step follows from the Dominated Convergence Theorem, which applies because, by Lemma 1.3.1 of Embrechts et al. (1997),

$$\frac{\int_{zt}^{t}\overline{F}_k(t-x)F_i^*(\mathrm{d}x)}{P(S>t)}\le\frac{P(X_k+X_i^*>t)}{P(S>t)}\sim\frac{\overline{F}_k(t)+\overline{F}_i^*(t)}{P(S>t)}.$$

Due to relation (37), the term above is bounded and integrable over $z\in(0,1]$.

Besides,

$$\begin{aligned} I_{22}(t) &\le \int_{t-t_0}^{t} P(S>t\,|X_i=x)F_i(\mathrm{d}x)\\ &= P(S>t, t-t_0<X_i\le t)\\ &\le P(t-t_0<X_i\le t)\\ &= \overline{F}_i(t-t_0)-\overline{F}_i(t)\\ &= o(1)P(S>t). \end{aligned}$$

The above inequality, together with (38), implies $I_2(t)=o(1)P(S>t)$.

Next, we turn to $I_3(t)$. For any $\delta\in(0,1)$, we have

$$\begin{aligned} I_3(t) &= \int_0^1\int_t^\infty P\left(S\ge\frac{x}{z}\middle|X_i=x\right)F_i(\mathrm{d}x)\,\mathrm{d}z\\ &= \int_0^{1-\delta}\int_t^\infty P\left(S-X_i\ge\left(\frac{1}{z}-1\right)x\middle|X_i=x\right)F_i(\mathrm{d}x)\,\mathrm{d}z\\ &\quad+\int_{1-\delta}^1\int_t^\infty P\left(S-X_i\ge\left(\frac{1}{z}-1\right)x\middle|X_i=x\right)F_i(\mathrm{d}x)\,\mathrm{d}z\\ &=: I_{31}(t)+I_{32}(t). \end{aligned}$$

Let $M = \sup_{1\le i\le n}|h_i|$. For t large, we have

$$\begin{aligned} I_{31}(t) &\le \int_0^{1-\delta}\int_t^{\infty} P\left(S - X_i \ge \frac{\delta t}{1-\delta}\,\middle|\, X_i = x\right) F_i(\mathrm{d}x)\,\mathrm{d}z \\ &\le (1+\varepsilon)\sum_{k=1,k\neq i}^{n}\int_0^{1-\delta}\int_t^{\infty} h_i(x)\overline{F}_k\left(\frac{\delta t}{1-\delta}\right) F_i(\mathrm{d}x)\,\mathrm{d}z \\ &\le (1+\varepsilon) M\overline{F}_i(t)\sum_{k=1,k\neq i}^{n}\overline{F}_k\left(\frac{\delta}{1-\delta}t\right), \end{aligned}$$

where the second inequality holds due to (35). It is easy to see that $I_{31}(t) = o(1)P(S>t)$. Moreover, for t large,

$$I_{32}(t) = \int_{1-\delta}^{1}\int_t^{\infty} P\left(S - X_i \ge \left(\frac{1}{z}-1\right)x\,\middle|\, X_i = x\right) F_i(\mathrm{d}x)\,\mathrm{d}z \;\le\; \delta\overline{F}_i(t).$$

Letting $\delta\to 0$, we obtain $I_3(t) = o(1)P(S>t)$. This completes the proof. □

To prove Theorem 5.6, let us start by considering a simpler two-dimensional case, which will play an important auxiliary role in establishing the desired result in higher dimensions.

Lemma A.1. *Let $\mathcal{N} = \{1,2\}$ in condition ($\mathbf{C}_5$). Then*

$$\lim_{q\uparrow 1}\tilde{r}_{i,q} = \frac{c_i}{c_1+c_2}, \qquad i\in\mathcal{N}.$$

Proof. We prove for $i=1$ only and the result for $i=2$ follows immediately. Note that equations (28) and (29) still hold. Obviously,

$$\begin{aligned} E\left(R_1\,|\,S>t\right) &= \int_0^1 \frac{P\left(X_1 > zS, S>t\right)}{P\left(S>t\right)}\mathrm{d}z \\ &= \int_0^1 \frac{P\left(X_1 > zX_2/(1-z), X_1+X_2>t\right)}{P\left(S>t\right)}\mathrm{d}z \\ &= \int_0^{\infty}\frac{1}{(1+w)^2}\frac{P\left(X_1>wX_2, X_1+X_2>t\right)}{P\left(S>t\right)}\mathrm{d}w, \end{aligned} \tag{39}$$

where the last step follow from a change of variable $w = z/(1-z)$ in the integration.

We claim that the probability $P\left(X_1>wX_2, X_1+X_2>t\right)$ is asymptotically equivalent to $\overline{F}_1(t)$ for every $w\in(0,\infty)$ and now prove the claim. For every fixed $w>0$, by the proof of Lemma 2.1 of Mitra and Resnick (2009), it holds for some $M > \max\{L_{12}, L_{12}/w\}$ that

$$\frac{1}{\overline{F}_1(t)}P\left(\left(\frac{X_1-t}{a(t)}, \frac{X_2}{a(t)}\right)\in\cdot\right) \xrightarrow{\mathrm{v}} \mu_1 \quad \text{in } \mathbb{M}_+\left([-M,\infty]\times[-\infty,\infty]\right), \tag{40}$$

where $\mathbb{M}_+([-M,\infty]\times[-\infty,\infty])$ is the set of all nonnegative Randon measures on $[-M,\infty]\times[-\infty,\infty]$ and the Radon measure μ_1 is defined as $\mu_1(\mathrm{d}x_1,\mathrm{d}x_2)=e^{-x_1}\mathrm{d}x_1\varepsilon_0(\mathrm{d}x_2)$, where ε_0 denotes the Dirac measure. Now, for fixed $w>0$ and $M>0$ given above, split the probability in the numerator of equation (39) as follows:

$$\begin{aligned}
&P(X_1>wX_2,X_1+X_2>t)\\
&=P(X_1>wX_2,X_1+X_2>t,X_1>t-Ma(t))+P(X_1>wX_2,X_1+X_2>t,X_1\le t-Ma(t))\\
&=:I_1(t)+I_2(t).
\end{aligned}$$

Note that

$$\begin{aligned}
I_2(t)&=P(X_1>wX_2,X_1+X_2>t,X_1\le t-Ma(t),X_2>Ma(t))\\
&\le P(X_1>wX_2,X_2>Ma(t))\\
&\le P(X_1>L_{12}a(t),X_2>L_{12}a(t))\\
&=o\left(\overline{F}_1(t)\right),
\end{aligned}$$

where in the second last step, we used the fact that $M>\max\{L_{12},L_{12}/w\}$. For $I_1(t)$, write

$$\begin{aligned}
I_1(t)&=P(X_1>wX_2,X_1+X_2>t,X_1>t-Ma(t),X_2\le Ma(t))\\
&\quad+P(X_1>wX_2,X_1+X_2>t,X_1>t-Ma(t),X_2>Ma(t))\\
&=I_{11}(t)+I_{12}(t).
\end{aligned}$$

Obviously, we have $I_{12}(t)\le P(X_1>wMa(t),X_2>Ma(t))=o\left(\overline{F}_1(t)\right)$. Moreover, with $A=\{(x_1,x_2)\in\mathbb{R}^2:x_1+x_2>0,x_1>-M,x_2\le M\}$,

$$\begin{aligned}
\lim_{t\to\infty}\frac{I_{11}(t)}{\overline{F_1}(t)}&=\lim_{t\to\infty}\frac{1}{\overline{F_1}(t)}P(X_1>wX_2,X_1+X_2>t,X_1>t-Ma(t),X_2\le Ma(t))\\
&=\lim_{t\to\infty}\frac{1}{\overline{F_1}(t)}P(X_1+X_2>t,X_1>t-Ma(t),X_2\le Ma(t))\\
&=\lim_{t\to\infty}\frac{1}{\overline{F_1}(t)}P\left(\left(\frac{X_1-t}{a(t)},\frac{X_2}{a(t)}\right)\in A\right)\\
&=\mu_1(A)\\
&=\int_0^\infty e^{-x_1}\mathrm{d}x_1\\
&=1,
\end{aligned}$$

where in the second step, we used the fact that $t - Ma(t) \geq wMa(t)$ for t large enough; in the fourth step, we used the vague convergence in equation (40); and in the second last step, we used the fact that μ_1 concentrates on the x-axis only.

In summary, we have established the claim regarding the asymptotic equivalence between $P(X_1 > wX_2, X_1 + X_2 > t)$ and $\overline{F}_1(t)$ for every $w \in (0,\infty)$. By equation (39), we have

$$\begin{aligned}
\lim_{q\uparrow 1} \tilde{r}_{1,q} &= \lim_{t\to\infty} E(R_1 | S > t) \\
&= \lim_{t\to\infty} \int_0^\infty \frac{1}{(1+w)^2} \frac{P(X_1 > wX_2, X_1 + X_2 > t)}{P(S > t)} \mathrm{d}w \\
&= \int_0^\infty \frac{1}{(1+w)^2} \lim_{t\to\infty} \frac{P(X_1 > wX_2, X_1 + X_2 > t)}{P(S > t)} \mathrm{d}w \\
&= \frac{c_1}{c_1 + c_2} \int_0^\infty \frac{1}{(1+w)^2} \lim_{t\to\infty} \frac{P(X_1 > wX_2, X_1 + X_2 > t)}{\overline{F}_1(t)} \mathrm{d}w \\
&= \frac{c_1}{c_1 + c_2} \int_0^\infty \frac{1}{(1+w)^2} \mathrm{d}w \\
&= \frac{c_1}{c_1 + c_2},
\end{aligned}$$

where we used the Dominated Convergence Theorem in the second step. The proof is now completed. □

Proof of Theorem 5.6. Suppose $n > 2$, and write $S_{-i} = S - X_i$. We prove the assertion by showing that S_{-i} and X_i, regarded as two risks, satisfy the conditions for X_1 and X_2 in Lemma A.1, respectively.

First, by Corollary 2.2 of Mitra and Resnick (2009),

$$P(S_{-i} > t) \sim \sum_{k=1, k\neq i}^{n} P(X_k > t) \sim \sum_{k=1, k\neq i}^{n} c_k \overline{F}_1(t),$$

where $\sum_{k=1,k\neq i}^{n} c_k \geq c_1 = 1$. Hence, because of the closure of MDA(Λ) under tail equivalence, S_{-i} is also in MDA(Λ). This implies the distribution of S_{-i} has an auxiliary function, say, $\tilde{a}(t)$, that is asymptotically equivalent to $a(t)$. Moreover, we obviously have $P(X_i > t)/P(S_{-i} > t) \to c_i / \sum_{k=1,k\neq i}^{n} c_k \geq 0$.

Second, we show that, for every $x > 0$,

$$P(X_i > x\tilde{a}(t), S_{-i} > t) = o(1) P(S_{-i} > t) \qquad \text{and} \qquad P(X_i > t, S_{-i} > x\tilde{a}(t)) = o(1) P(S_{-i} > t).$$

The first equation above is a consequence of Lemma 3.4 of Asimit et al. (2011), the asymptotic equivalence between

$\tilde{a}(t)$ and $a(t)$, and the tail equivalence between X_1 and S_{-i}. The other equation holds because

$$\begin{aligned}\frac{P(X_i>t,S_{-i}>x\tilde{a}(t))}{\overline{F}_1(t)} &\le \frac{1}{\overline{F}_1(t)}P\left(X_i>t,\bigcup_{k=1,k\neq i}^{n}\left\{X_k>\frac{x\tilde{a}(t)}{n-1}\right\}\right)\\ &\le \sum_{k=1,k\neq i}^{n}\frac{1}{\overline{F}_1(t)}P\left(X_i>t,X_k>\frac{x\tilde{a}(t)}{n-1}\right)\\ &\to 0,\end{aligned}$$

where the first step is due to the nonnegativity of the risks, and the last step follows from the asymptotic equivalence between $\tilde{a}(t)$ and $a(t)$.

Third, we shall prove that there exists $L_i>0$, such that

$$P(X_i>L_i\tilde{a}(t),S_{-i}>L_i\tilde{a}(t))=o(1)P(S_{-i}>t). \tag{41}$$

Let $L_i=(n-1)\max_{j,k\in\mathcal{N},j\neq k}L_{jk}$. We have

$$\begin{aligned}\frac{P(X_i>L_i\tilde{a}(t),S_{-i}>L_i\tilde{a}(t))}{\overline{F}_1(t)} &\le \frac{P\left(X_i>L_i\tilde{a}(t),\bigcup_{k=1,k\neq i}^{n}\left(X_k>\max_{j,k\in\mathcal{N},j\neq k}L_{jk}\tilde{a}(t)\right)\right)}{\overline{F}_1(t)}\\ &\le \sum_{k=1,k\neq i}^{n}\frac{P\left(X_i>L_i\tilde{a}(t),X_k>\max_{j,k\in\mathcal{N},j\neq k}L_{jk}\tilde{a}(t)\right)}{\overline{F}_1(t)}\\ &\to 0,\end{aligned}$$

where the first step is due to the nonnegativity of $\boldsymbol{X}$, and the last step is due to condition ($\mathbf{C}_5$) and the asymptotic equivalence between $\tilde{a}(t)$ and $a(t)$. Equation (41) holds since X_1 and S_{-i} are tail equivalent.

Collectively, we have shown that S_{-i} and X_i satisfy all the assumptions in the two-risk case as described in Lemma A.1, and thus we readily obtain

$$\lim_{q\uparrow 1}\tilde{r}_{i,q}=\frac{c_i/\sum_{k=1,k\neq i}^{n}c_k}{1+c_i/\sum_{k=1,k\neq i}^{n}c_k}=\frac{c_i}{\sum_{k=1}^{n}c_k}.$$

This completes the proof. □

Appendix B Technical calculations for the example in the numerical section

This section details the calculations needed to derive the limits of the CTE-based and GTE-based allocations, which are identical and given in (15). To this end, we focus on the limit of $\tilde{r}_{1,q}$ as $q\uparrow 1$, and the limit of $\tilde{r}_{2,q}$ can be obtained

via $\lim_{q\uparrow 1}\tilde{r}_{2,q} = 1 - \lim_{q\uparrow 1}\tilde{r}_{1,q}$.

With (19) and (26), the limit measure μ in condition ($\mathbf{C}_1$) as well as Theorem 4.2 can be evaluated via (Asimit et al., 2011; Tang and Yuan, 2013):

$$\mu(\boldsymbol{x},\boldsymbol{\infty}) = x_1^{-\alpha} + bx_2^{-\alpha} - \left(x_1^{-\alpha\beta} + b^{\beta}x_2^{-\alpha\beta}\right)^{1/\beta},$$

where $b = (\lambda_2/\lambda_1)^{\alpha}$ and $\boldsymbol{x} \in \mathbb{R}_+^2$. Let us rewrite the limit in (15) as

$$\begin{aligned}&\int_0^1 \frac{\mu(\boldsymbol{x} \in [\mathbf{0},\boldsymbol{\infty}) : x_1 > x_2 z/(1-z), x_1 + x_2 > 1)}{\mu(\boldsymbol{x} \in [\mathbf{0},\boldsymbol{\infty}) : x_1 + x_2 > 1)}\,\mathrm{d}z \\ &= 1 - \int_0^1 \frac{\mu(\boldsymbol{x} \in [\mathbf{0},\boldsymbol{\infty}) : x_2 > x_1 (1-z)/z, x_1 + x_2 > 1)}{\mu(\boldsymbol{x} \in [\mathbf{0},\boldsymbol{\infty}) : x_1 + x_2 > 1)}\,\mathrm{d}z. \end{aligned} \tag{42}$$

For $\boldsymbol{x} \in \mathbb{R}_+^2$, define

$$\mu_1(\boldsymbol{x}) = -\frac{\partial}{\partial x_1}\mu(\boldsymbol{x},\boldsymbol{\infty}) = \alpha x_1^{-\alpha-1}\left[1 - \left(x_1^{-\alpha\beta} + b^{\beta}x_2^{-\alpha\beta}\right)^{1/\beta-1} x_1^{\alpha(1-\beta)}\right].$$

To compute the denominator in the integration in (42), we have

$$\begin{aligned}\mu(\boldsymbol{x} \in [\mathbf{0},\boldsymbol{\infty}) : x_1 + x_2 > 1) &= \mu\big(\boldsymbol{x} \in [\mathbf{0},\boldsymbol{\infty}) : x_1 > 1\big) + \mu\big(\boldsymbol{x} \in [\mathbf{0},\boldsymbol{\infty}) : x_1 \in [0,1], x_1 + x_2 > 1\big) \\ &= 1 + \int_0^1 \mu_1(s, 1-s)\,\mathrm{d}s,\end{aligned}$$

where the second term is calculated numerically. Now consider the numerator in (42). For $z \in (0,1)$, we have

$$\begin{aligned}&\mu(\boldsymbol{x} \in [\mathbf{0},\boldsymbol{\infty}) : x_2 > x_1 (1-z)/z, x_1 + x_2 > 1) \\ &= \mu\big(\boldsymbol{x} \in [\mathbf{0},\boldsymbol{\infty}) : x_1 > 1\big) + \mu\big(\boldsymbol{x} \in [\mathbf{0},\boldsymbol{\infty}) : x_1 \in [0,z), x_2 > x_1 (1-z)/z\big) \\ &\quad + \mu\big(\boldsymbol{x} \in [\mathbf{0},\boldsymbol{\infty}) : x_1 \in [z,1], x_2 > 1 - x_1\big) \\ &= 1 + \int_0^z \mu_1(s, s(1-z)/z)\,\mathrm{d}s + \int_z^1 \mu_1(s, 1-s)\,\mathrm{d}s,\end{aligned}$$

where the last two terms can be readily computed using numerical integration.